NTT Technical Review

7
2011

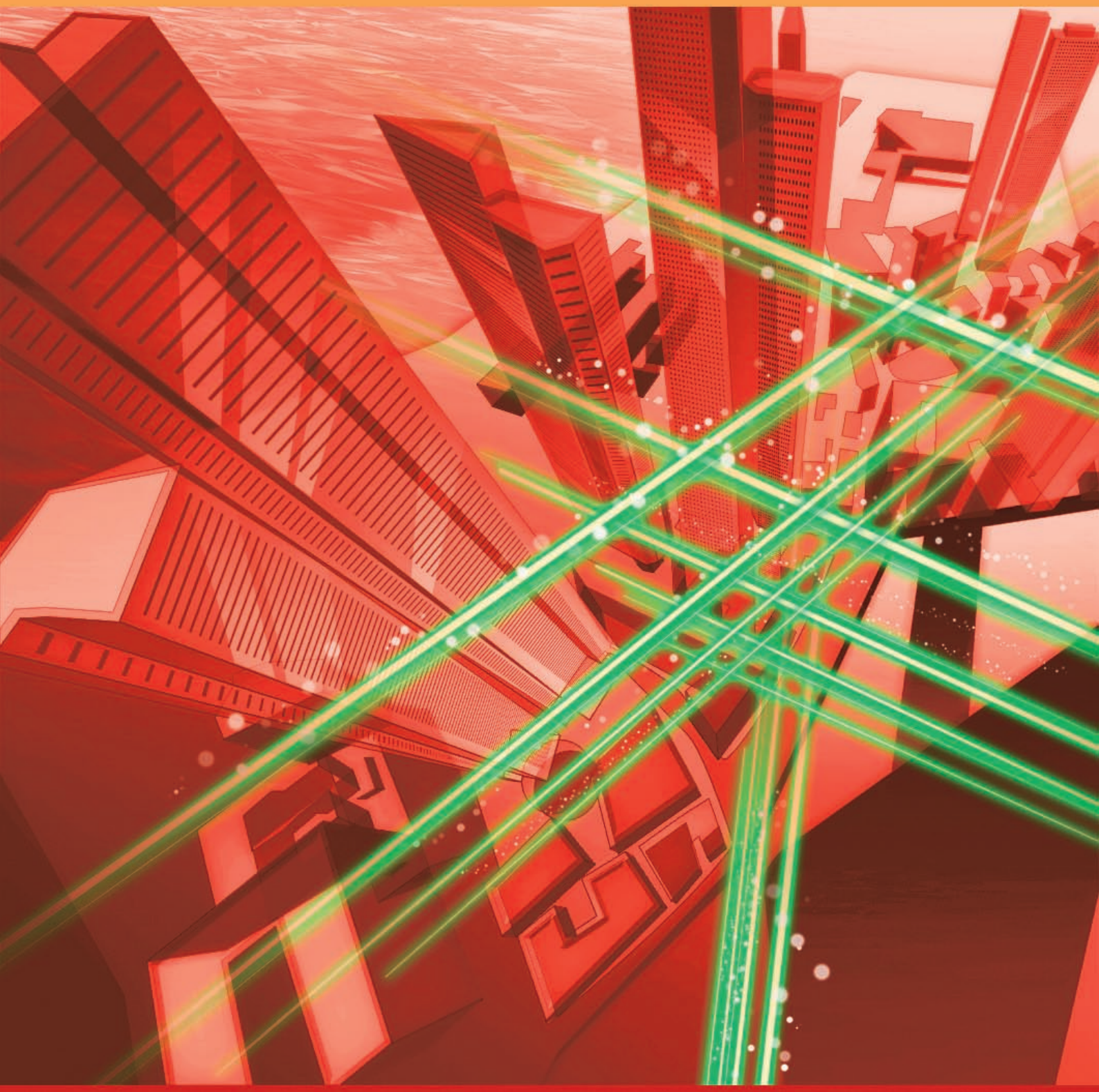

July 2011 Vol. 9 No. 7

NTT Technical Review

July 2011 Vol. 9 No. 7

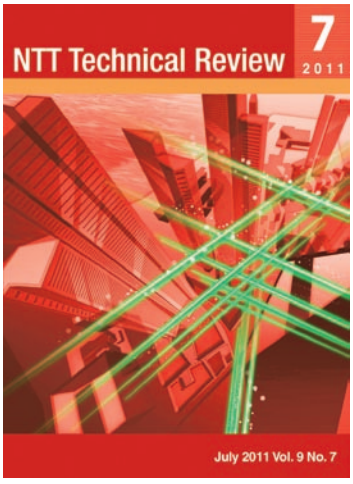

Toward the Ultimate in Optical Integration Technology

Masaya Notomi
Senior Distinguished Scientist,
NTT Basic Research Laboratories

Photonic crystal, which can function as a photonic insulator (something not found in nature), is expected to provide major breakthroughs in optical integration technology. Dr. Masaya Notomi, Senior Distinguished Scientist at NTT Basic Research Laboratories, is a driving force behind research that aims to achieve on-chip optical networks by applying the special properties of photonic crystal. We asked him about his research experiences and what led him to take up the challenges of photonics.

Photonic crystal: achieving optical integrated circuits

—Dr. Notomi, could we begin by hearing about the research that you are now pursuing?

I am now researching the creation of structures called photonic crystals using nanofabrication techniques with the aim of developing optical large-scale integration technologies that have so far been difficult to achieve. A major objective of this research is to resolve problems in existing electronics technologies by introducing genuine photonic network technologies in information-processing chips.

In electronic circuits, the more you raise performance the more you increase energy consumption and heat. In optics, however, increasing processing speed causes almost no increase in energy consumption. In other words, the energy consumption and heat generation can be minimized by introducing optics-based processing in circuits. With this in mind, researchers are attempting to incorporate optical wiring and circuits into electronic circuits using a variety of methods.

To begin with, achieving large-scale integrated circuits by optical means inside a chip requires the fabrication of devices and wires (that is, optical waveguides) whose structures completely confine light. It also requires that the size of individual devices and wires be exceedingly small to achieve large-scale integration. In this regard, photonic crystal can function as a *photonic insulator* and confine light in a very small space, which makes it applicable to the fabrication of optical integrated circuits. By the way, although there are a number of naturally occurring insulators that block the flow of electricity, no photonic insulators exist in nature. The artificial structure of photonic crystal makes it possible to achieve photonic insulators for the first time.

Furthermore, in the processing of signals for a logic operation in information-processing circuits, some packet signals must be made to wait until the others arrive so that the computation can be performed. To date, however, optical circuits have been incapable of making optical signals wait, and this has been one of their weak points. Photonic crystals, however, can significantly slow down the propagation speed of light. In the laboratory, we have been successful in using photonic crystal to produce extremely slow light with a speed about 1/50,000 that of ordinary

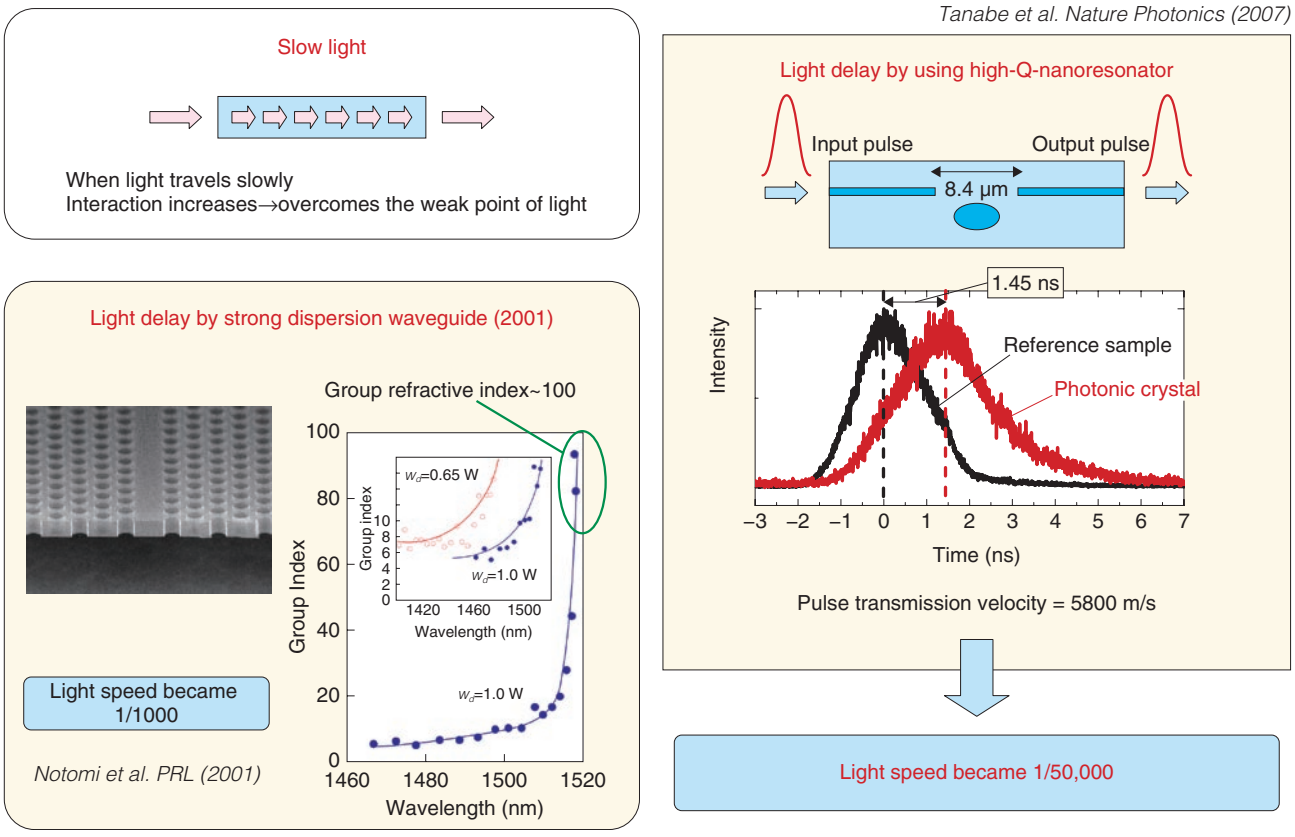

Fig. 1. Strange nature of photonic crystal: slow light.

light (**Fig. 1**).

Photonic crystal has various peculiar properties in addition to *slow light*. One example is the phenomenon of *negative refraction* whereby the refractive index is made negative by using a special type of photonic crystal (**Fig. 2**). In the natural world, the refractive index is positive for all substances, but a negative value can lead to unexpected and interesting phenomena. For example, a simple flat surface can function as a lens if it has a negative refractive index.

Ongoing innovation in optical technologies

—What kinds of results is your research team currently aiming for?

One use of photonic crystal that we have been thinking about is the development of *ultralow-energy and ultrasmall high-performance optical devices* for use in information-processing equipment. Up to now, the large amount of power consumed by microprocessor units (MPUs), for example, has prevented them from being incorporated into compact information-processing equipment such as mobile phones. The characteristics of electronic circuits inside MPUs are such that the energy cost of information transfer increases with the bit rate, which means that it is difficult to significantly reduce power consumption while raising processing capacity. However, if we could incorporate optical technologies into MPUs, the energy cost of information transfer would not increase for higher bit rates, which should make it possible to drive circuits by using much less power than in the case of electronic devices even as processing speed increases. In our research, we have already demonstrated that photonic crystal can be used to drastically reduce operating energy in a number of optical devices (**Fig. 3**).

In addition to low power consumption, another requirement here is the integration of individual devices. Our aim is to develop optical integration technologies so that we can achieve optical integrated circuits while maintaining this energy-saving effect.

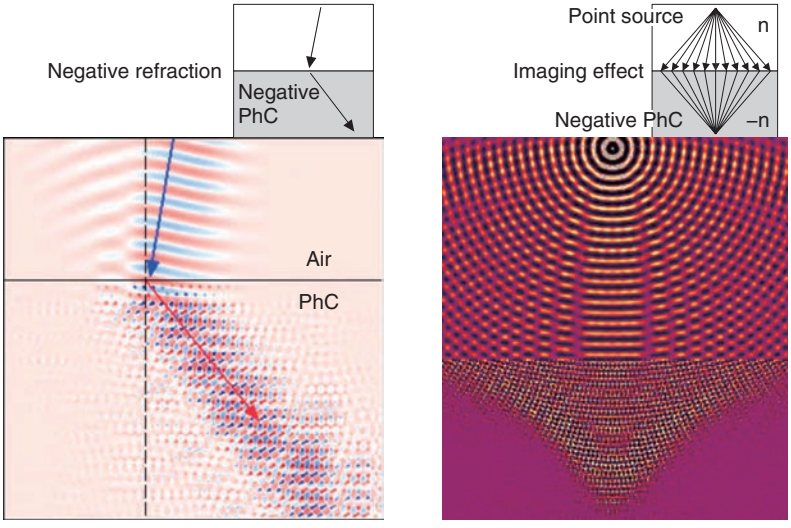

PhC: photonic chrystal

Fig. 2. Strange nature of photonic crystal: negative refraction.

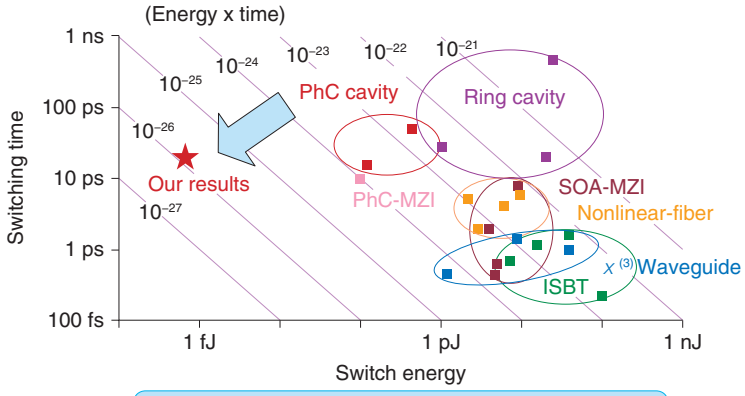

MZI: Mach-Zehnder interferometer
SOA: semiconductor optical amplifier
ISBT: intersubband transition

Fig. 3. Operation speed versus energy consumption.

Research on photonic crystals is still at the fundamental level, but we can expect optical integration technologies—if successfully developed—to be applied to commercial products sometime in the future.

At the same time, high-precision photonic crystals will be needed to fabricate high-quality optical devices, and the key to this is the development of advanced fabrication techniques. Over the ten years that our team has been in existence, we have been making steady improvements in the performance of photonic crystal and have been working to improve our fabrication techniques. It is acknowledged that NTT has been able to fabricate high-quality photonic-crystal waveguides from an early stage because of these efforts. Establishing high-precision fabrication

techniques is extremely important for later research.

Looking back at the history of electronic circuits, we can see how vacuum tubes were followed by transistors and how technologies for integrating transistors on a chip were developed by Intel and other companies. In a similar way, innovations in optical technologies are now appearing one after another. Up to now, only individual optical devices could be developed, but their evolution toward integrated optical circuits is beginning.

If fabrication techniques continue to progress, we can expect optical technologies to somehow be incorporated into chips in about ten years time. I believe that photonic-crystal technology will play an important role in this evolution.

Adoption of a new theme and formation of a cross-organization team in caravan form

—Could you tell us about the path that you took to your current research endeavors?

During my university days, I researched the peculiar behavior of electrons confined to one-dimensional states by synthesizing crystals having a pseudo one-dimensional structure and cooling them to extremely low temperatures. Then, after joining NTT Laboratories in 1988, I undertook research on structures that could confine electrons to one-dimensional or even zero-dimensional states with particular application to optical devices. At that time, my superiors in this research group were being transferred, and in the end, I came to continue this research on my own. I was still just a new, young researcher, and there was not much of a budget, but upon looking back, I could say that this was a research environment that gave me much freedom.

After performing this research for about ten years, I had written a number of papers and had completed enough research to write my doctoral thesis. It was at that time that my superior asked me what I thought about changing research theme. He was also very generous in telling me that "Whatever you do is fine so please select a new theme of your own choice." I then spent about one year in Sweden as a visiting researcher during which time I completed my doctoral thesis and thought about my next research theme.

Around that time, photonic crystal research was passing from the concept phase to the testing of operating principles using microwaves. While I was in Sweden, such testing in the optical wavelength region began. In Japan, photonic crystal research had begun only in some universities, but the worldwide number of researchers involved in this field was starting to climb.

Moreover, the photonic crystals were relatively large structures with feature dimensions greater than 100 nm, which was about one order of magnitude larger than the structures that I had fabricated in past research. Such a large structure was technically easy to fabricate. Taking all of this into consideration, I decided that photonic crystals would be my next research theme.

At that time, I also hatched a plan to shift from individual research as I had been doing to research that I would perform with fellow researchers. We called this our *caravan* plan in which we would recruit researchers with an interest in photonic crystals not only from the organization to which I belonged but also from other research laboratories.

This does not mean to say that many researchers suddenly offered to participate, but people from several groups started to express interest and I was eventually able to form a cross-organization team. At NTT Laboratories, there is actually a lot of interdisciplinary research, but most of this involves the development of practical products over a two- or three-year period. Fundamental research themes like the one that we were pursuing with photonic crystals were actually quite rare. This cross-organization team was able to conduct research on photonic crystals using fabrication and measurement techniques that were not previously available, which I believe had a great effect on results.

Pushing yourself into a state conducive to inspiration

—Please tell us about your current research team.

At present, there are seven members from the same research laboratory and several members from other laboratories. Our research on photonic crystals is broken down into several themes with several members dealing with each. Of utmost concern here is that each and every theme should be something that will grow over time. For this reason, I leave everyday research to team members, but I think about medium- and long-term research themes by forecasting the state of development several years in the future and then working backwards to the present.

Looking for a theme on one's own from a blank slate is certainly not unpleasant, but there is pressure

just the same. And the fact is that, if you don't push yourself into such a state, you cannot expect inspiration or novel ideas to form. Pushing oneself mentally, though, is not necessarily fun. When I find myself in such a situation, I think back to my experiences as a visiting researcher in Sweden, when I would think every day about what I should be researching. Those experiences are proving to be quite useful even today. I am also very grateful to my superior who gave me the time to ponder my next move.

Research work, though, is often a matter of trial and error and also of detours as researchers grope for answers. Consequently, there must be some margin and flexibility in the time, people, and organizations specified for a research project to prevent researchers from coming to a standstill. In this regard, I think that researchers at NTT Laboratories are fortunate to be working in an environment conducive to basic research.

Traveling to Tibet alone

—Do you have any hobbies or interests outside of research?

Yes, I do. After entering the workforce and while I was still single, I would often travel by myself to places overseas. I first travelled to popular destinations in North America and Europe, for example, but in time, I got bored with such trips, and I eventually started to visit countries like Tibet, India, and Vietnam.

I thought that Tibet, in particular, was fascinating, and my trip to Lake Namtso (or Gnam-mtso) in the highlands of Tibet left a strong impression on me. This lake is located in a rural area several hundred kilometers from the capital; there are no roads leading up to it, so it cannot be accessed by normal modes of transportation. But wanting to go there, I gathered some information after arriving in Tibet, and I found that I could charter a jeep. The driver and I set out in the direction of the lake with no roads to go by. After much difficulty, we eventually arrived. I thought that Lake Namtso was too beautiful for this world. Situated at an elevation of 4718 m, it is the highest salt lake in the world. This lake is so magnificent that it is proudly called the "sacred lake" or the "lake nearest to heaven" in the Tibetan language (**Photo 1**).

After I got married and had children, my solo trips came to an end, but I still love to walk around town. On my days off, I often take my kids with me on walks to temples, art galleries, and other interesting places.

Photo 1. Lake Namtso, Tibet.

Becoming a better researcher by understanding your research theme

—Dr. Notomi, could you please leave us with some advice for young researchers?

I would be happy to. First of all, it is helpful to have staying power over the long term with respect to one's research theme. All researchers, myself included, can lose spirit if research results do not turn out as expected. But that's when you must have the fortitude to withstand such painful periods and not give up. This is something that I tell myself all the time.

Secondly, you must discover for yourself what it is about your research theme that is interesting or exciting. If you don't develop on your own a deep understanding of the possibilities behind your research theme and what that theme might mean to the field in question, you will never discover just how interesting your research theme can be. And if you can't discover that, you will not be able to continue your research over the long term.

It is relatively easy to get a budget for research that is currently fashionable, and in recent years, even university students have been switching over to such research in great numbers. I guess some researchers are worried that they will be left behind if they don't get on board immediately with such fashionable research. However, I feel that this kind of impatience in research can be very dangerous. This is because most of research is a series of failures, but that does not mean to say that there are no successes, few though they may be. Researchers must continue to research while accumulating the results of those

successful experiments over time. Even if failures should continue, researchers that can discover on their own the fascinating aspects of their research should be able to use those experimental failures to get on a path toward success. In this way, researchers should be able to continue researching without getting discouraged even if successes are few and far between.

In this sense, I believe that *discovering what is exciting in your research by yourself* is an important qualification for a researcher.

Masaya Notomi

Senior Distinguished Scientist, Group Leader, Photonic Nanostructure Research Group, NTT Basic Research Laboratories.

He received the B.E., M.E., and Dr.Eng. degrees in applied physics from the University of Tokyo in 1986, 1988, and 1997, respectively. He joined NTT Optoelectronics Laboratories in 1988. Since then, his research interest has been to control the optical properties of materials and devices by using artificial nanostructures. He has been in NTT Basic Research Laboratories since 1999. During 1996–1997, he was a visiting researcher at Linköping University in Sweden. He was a guest associate professor in the Department of Applied Electronics at Tokyo Institute of Technology (2003–2009) and is currently a guest professor in the Department of Physics at Tokyo Institute of Technology. He received the 2006–2008 IEEE/LEOS Distinguished Lecturer Award, JSPS (Japan Society for the Promotion of Science) Prize in 2009, the Japan Academy Medal in 2009, and the Commendation for Science and Technology from the Minister of Education, Culture, Sports, Science and Technology (Prize for Science and Technology, Research Category) in 2010. He is a member of the Japan Society of Applied Physics, the American Physical Society, the Optical Society of America, and IEEE.

Simulation System for Estimating Hazardous Voltages Induced in Telecommunication Cables by Power Faults

Abstract

This article introduces a system for simulating hazardous voltages induced in telecommunication cables in the event of power faults in high-voltage power transmission systems. When the estimated induction voltages exceed human safety limits, mitigation measures such as shielding the cables and using insulation (including the replacement of metallic telecommunication cable by optical fiber) are required. However, to date most of the work of calculating and estimating induced voltages has depended on manual operations. The new simulation system greatly reduces most of the manual operations by using a personal computer and a telecommunication cable database.

1. Introduction

Power faults in high-voltage power transmission lines can be caused by lightning, typhoons, and power-line insulation breakdown, as shown in **Fig. 1**. Figure 1(a) shows a power fault current flowing to the ground after a power fault was caused by lightning. Figure 1(b) shows the mechanism of power induction

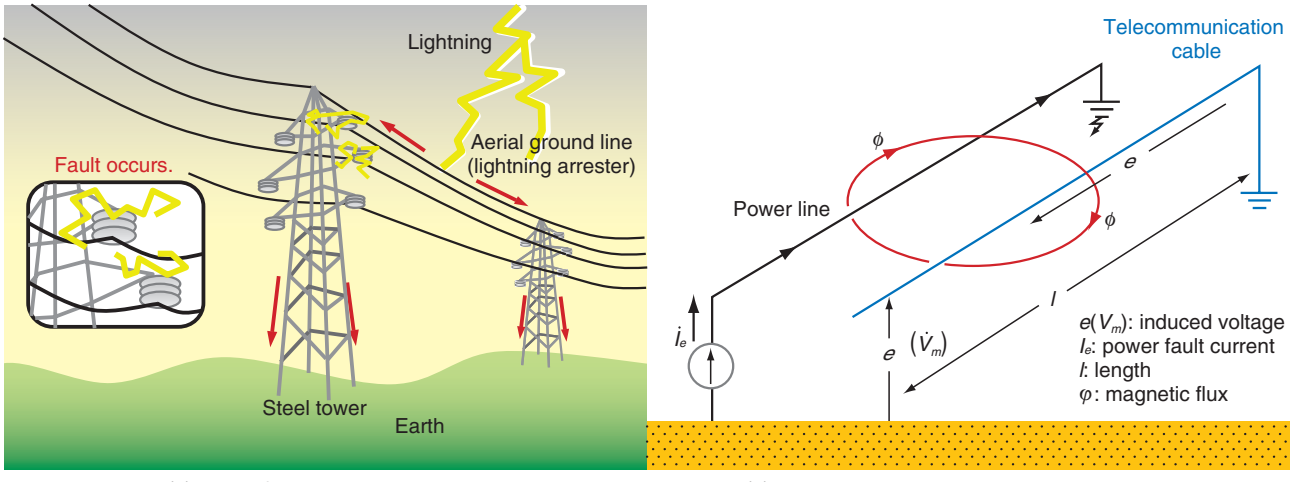

(a) Power fault caused by lightning

(b) Power induction in telecommunication cables

Fig. 1. Power fault in high voltage power transmission lines.

† NTT EAST
Ota-ku, 144-0053 Japan

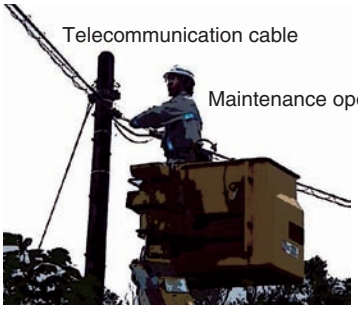

Photo. 1. Electric shock risk to maintenance operators.

between a power line and a telecommunication cable running parallel to it. When a power fault occurs, a high electromagnetic field can be generated by the power fault current. This field also generates electromagnetic induction ac (alternating current) voltages in the telecommunication cable. When a maintenance operator touches the telecommunication cable, as shown in **Photo 1**, after a power fault has occurred, the operator receives a shock from the ac voltage induced in the telecommunication cable. The induced voltage causes ac to flow through the operator's body, typically via a hand. Such an electric shock can cause secondary accidents such as the operator being knocked over or falling to the ground and may even lead to death if the ac flow through the operator's heart exceeds the safety limits.

To ensure the safety of maintenance operators, NTT and electric power companies have agreed to establish countermeasures for hazardous voltages caused by power induction. These agreements prescribe the calculation of induced voltage beforehand and the implementation of countermeasures whenever the voltage exceeds the limits shown in **Table 1** [1]. The limits depend on the interruption time of the power fault. In the case of a high-stability power line having a short interruption time, the voltage induced in the telecommunication cable should be no more than 650 Vrms. In any case, the voltage induced in a telecommunication cable needs to be calculated beforehand, and if it exceeds the limits, countermeasures must be taken such as increasing the insulation on metallic cables, changing to a telecommunication cable with a high shielding effect, changing the routes of the telecommunication cables, or upgrading from metallic telecommunication cable to optical fiber.

2. Problems with existing calculation methods

To calculate voltages in telecommunication cables [2], we need the routes of power lines and telecommunication cables and also the power fault currents. The power line routes and power fault currents are given as paper-based maps and figures by the power companies. The telecommunication cable routes are obtained from NTT itself. The power-line and telecommunication-cable routes are on different maps, so these maps must be manually copied to a new map in order to obtain the distances between the power lines and telecommunication cables; this takes many hours per cable. Moreover, it has become increasingly difficult to build up knowledge about induced voltage calculation and induction countermeasures because employees with induction estimation skills are retiring and the in-house workforce is shrinking. This situation has generated a need for a tool that can estimate induced voltages simply while maintaining high accuracy.

3. Simulation system

Our new simulation system is compared with the existing method in **Fig. 2**. There are five steps in the procedure for obtaining induced voltage in telecommunication cables.

(1) Gather power-line and telecommunication-cable route information.

Table 1. Hazardous voltage limits in case of power fault.

Application conditions	Limiting value
High-stability power line having a continuous ground-fault current lasting no longer than 0.06 s	650 V
High-stability power line having a continuous ground-fault current lasting between 0.06 and 0.1 s	430 V
Other power lines	300 V

* A power line having a transmission voltage of 100 kV or greater, a low frequency of faults, and a fault interval no longer than 0.1 s

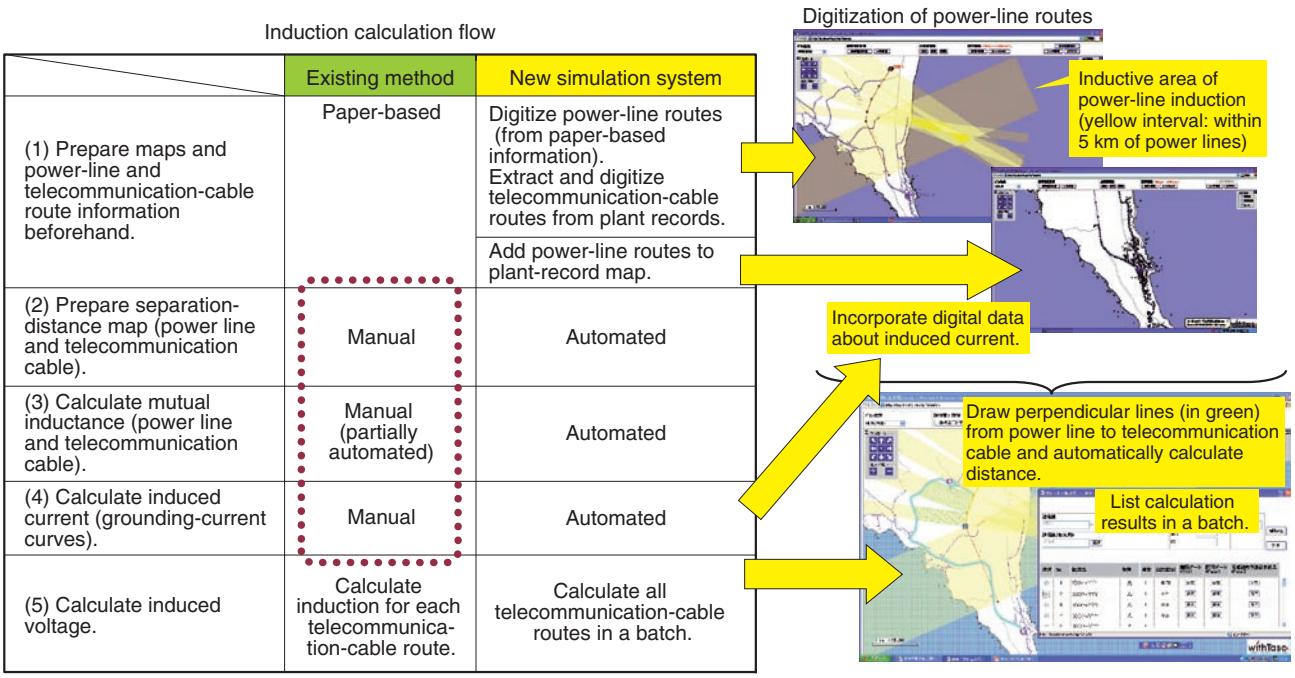

Fig. 2. Induction estimation flow and associated screen images.

(2) Make a distance map of the separations between power lines and telecommunication cables.
(3) Calculate mutual inductance between power lines and telecommunication cables from the distance map obtained in (2).
(4) Calculate the power fault current.
(5) Calculate the induced voltage.

In the existing method, steps (2)–(4) involve time-consuming manual operations. The maps of power lines and telecommunication cables are copied by hand, so high-level skills are required to reduce errors. When the number of telecommunication cable routes is high, e.g., 100 or 1000, it is hard to check all induced voltages for relevant telecommunication cables. By contrast, the new simulation system, which runs on a personal computer, is not based on manual operations and has three good characteristics: automatic preparation of the distances between a power line and telecommunication cables on the map, automatic calculation of induced voltage, and batch calculation of induction for all telecommunication-cable routes.

3.1 Automatic preparation of distances on map

The first step in the existing method is to acquire information about power-line routes (from paper maps) from the power company and manually overlay that information onto the NTT paper-based plant record. The next step is to project perpendicular lines from the power line to sections of the telecommunication cable using rulers and squares and to calculate the average distance for each section. By contrast, the new system enables power-line information on a paper map to be incorporated into an electronic telecommunication cable route database via a scanner and lets a user digitize coordinate data (latitude & longitude) of a power-line route by simply clicking on the route on a screen, thereby automating the creation of a map showing the distances between the power line and telecommunication cables (or routes). In this way, it is possible to automatically obtain a map of the separation distances along a power line (distance map), which in turn makes it possible to calculate mutual inductances between the power line and telecommunication cables automatically.

3.2 Automatic calculation of induced voltage

Voltage induced in the telecommunication cable can be calculated by multiplying induced current (grounding current) by mutual inductance as computed from the distance map. In the existing method, induced-current values are also provided by the

power company in the form of paper-based graphs. The new tool enables this graph data to be input into the system via a scanner so that induced-current values can be digitized by clicking on those data curves on the screen. This enables induced-current values needed for calculating induced voltage to be extracted automatically.

3.3 Batch calculation of induction for all telecommunication-cable routes

The new tool can also automatically determine whether any telecommunication-cable route is within the induction-impact range of a power line and simultaneously calculate induction for all telecommunication-cable routes in a batch. The operations needed to calculate and estimate induction can therefore be done much more efficiently. The precision of calculations is also improved through the use of map data that has not been input manually and is thus more accurate, which reduces the errors in induction estimation.

4. Conclusion

NTT has developed a powerful new simulation system for estimating induction with a focus on hazardous voltages induced in telecommunication cables by power faults in high-voltage power transmission lines. This simulation system enables power-line routing information needed for calculating induced voltage to be digitized, thereby reducing computation time and improving computational accuracy. As a result, it has become possible to respond promptly to plans for raising voltage in power transmission lines, reduce dispersion in calculation results, and make more accurate decisions about the need to implement countermeasures to power induction.

In fiscal year 2010, we used the results of field trials to improve the system's workability and operability, and in response to the wishes of NTT branch offices involved in this trial, we implemented a function for estimating induced voltage from multiple power transmission lines. We also plan to implement a function for estimating voltage induced by other types of power-transmission systems such as in electric railways in addition to power transmission lines and investigate the networking of the induction-estimation tool to make calculations more efficient and to link databases. Our objective is to implement these enhancements in the field beginning in fiscal year 2011.

References

[1] "Calculation Method to Estimate Electrostatic and Electromagnetic Induction in the Design of Telecommunication Facilities," NTT Technical Review, Vol. 5, No. 8, 2007.
https://www.ntt-review.jp/archive/ntttechnical.php?contents=ntr200708sf3.html

[2] "Induction (Vol. 1)," The Telecommunications Association, Tokai Division, p. 127, 1981 (in Japanese).

Fault Cases and Countermeasures for Field Assembly Connectors in Optical Access Facilities

Abstract

We have investigated faults with field assembly connectors that had been breaking down in optical access facilities. These faults were caused by fiber scratching, fracture of the mechanical splice part, incorrect fiber lengths, incorrect cleaving, incorrect joining, and so on. All these causes can be eliminated by countermeasures such as correct use of tools and proper procedures.

1. Introduction

NTT EAST and NTT WEST had more than 15.1 million customers using optical fiber broadband services (FLET'S HIKARI) at the end of March 2011. This rapid expansion has been accompanied by unexpected faults in optical access facilities. NTT EAST Technical Assistance and Support Center provides consultation on a variety of fault cases and strives to maintain a high-reliability network. This article introduces fault cases and countermeasures for field assembly connectors, which are used to join optical fibers in optical access facilities.

2. Field assembly connectors

A field assembly connector is composed of three main parts: the ferrule, mechanical splice, and clamp. There are several kinds of field assembly connectors such as the field assembly small-sized (FAS) connector. The connector assembly procedure has six steps as follows:

(1) Strip the 0.25-mm-diameter fiber coating from the optical fiber using a mechanical stripper.
(2) Clean the stripped fiber (bare fiber) with alcohol.
(3) Cut the bare optical fiber to the correct length using a fiber cleaver.
(4) Insert this bare optical fiber into the mechanical splice part inside the field assembly connector.
(5) Join it to the built-in optical fiber inside the ferrule.
(6) Fix the position of the bare optical fiber by releasing the wedge from the mechanical splice inside the connector.

† NTT EAST
Ota-ku, 144-0053 Japan

3. Fault cases with field assembly connectors

In fiscal year 2009, we investigated faults with field assembly connectors that had broken down in a certain region of Japan. The direct causes of the faults are summarized in **Fig. 1**. We also found that these connectors often have multiple causes in addition to the direct causes. All of the direct causes of connector faults are detailed below in order of occurrence frequency.

3.1 Fiber scratching

3.1.1 Fault cases

A scratch on an optical fiber can grow with time and eventually lead to fiber breakage. Examples of failures of this kind are shown in **Fig. 2**. Such scratches can be made when the sheath is removed from the optical fiber drop cable if the blades of the wire nippers damage the fiber. They can also be made when the fiber coating is removed from the coated optical fiber if coating debris from previous stripping was left on the blades of the mechanical stripper.

3.1.2 Countermeasures

(1) Remove the sheath carefully without the nipper blades damaging the optical fiber, as shown in

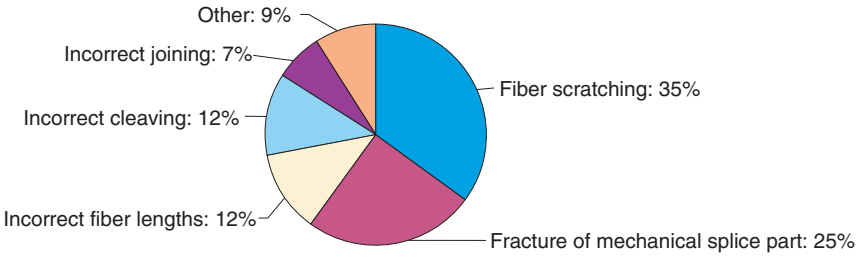

Fig. 1. Summary of fault causes.

(a) Scratching caused by nipper blades

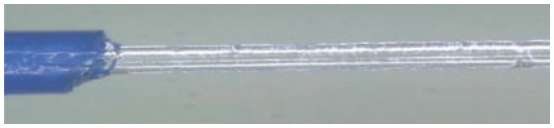

(b) Scratching caused by coating debris

Fig. 2. Examples of scratched optical fibers.

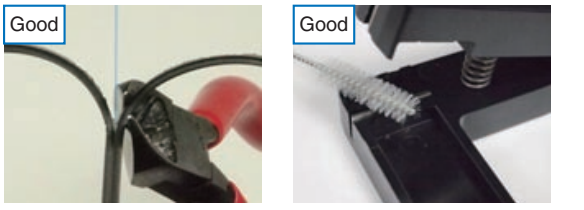

(a) Correct sheath removal (b) Cleaning before coating removal

Fig. 3. Countermeasures to fiber scratching.

Fig. 4. Fracture of the mechanical splice part.

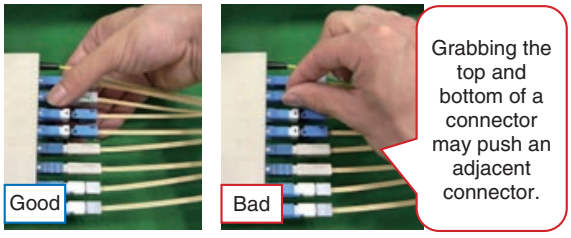

(a) Connector insertion/removal

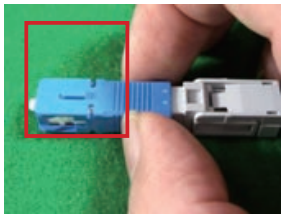

(b) Connector finger-grip

Fig. 5. Countermeasures to fracture of the internal mechanical splice part.

Fig. 3(a), so as not to scratch the fiber.

(2) Clean the mechanical stripper before removing the fiber coating, as shown in **Fig. 3(b)**.

3.2 Fracture of mechanical splice part

3.2.1 Fault cases

When an optical connector is carelessly inserted into or removed from equipment, lateral force can be accidently applied to an adjacent connector. This force can damage the mechanical splice part inside the connector and lead to fracture of this part **(Fig. 4)**. The fracture may result in fiber breakage. In addition, when the connector is inserted into or removed from equipment at an inclination to the optical connector adapter, force can be applied to the connector, which can cause the mechanical splice part to fracture.

3.2.2 Countermeasures

(1) Be careful not to push adjacent optical connectors **(Fig. 5(a))**. Hold the finger-grip of an optical connector correctly when inserting or removing it **(Fig. 5(b))**.

(2) Insert an optical connector into or remove one

from equipment horizontally with respect to the optical connector adapter.

3.3 Incorrect optical fiber length

3.3.1 Fault cases

Failure to set the optical fibers in the tools correctly can lead to an incorrect length and may result in fiber breakage or an increase in loss. Examples of incorrect optical fiber lengths are shown in **Fig. 6**.

3.3.2 Countermeasures

(1) Set the bare and coated optical fiber in the proper tools correctly.
(2) Use the scale marks on the fixture of the field assembly connector to measure the bare and coated optical fiber lengths before joining to the built-in optical fiber.

3.4 Incorrectly cleaved fiber end

3.4.1 Fault cases

If there are no problems with the fiber cleaver, the fiber will be cleaved correctly and have a correct, flat, and smooth end perpendicular to the fiber axis. However, if there are problems, the fiber end will have an incorrect and uneven end **(Fig. 7)**. An incorrectly cleaved fiber end can lead to abnormal joining to the built-in optical fiber and may result in an increase in loss. A fiber end can be incorrectly cleaved for several reasons. For example, the fiber end can be cleaved incorrectly with a dropped cleaver or one that has struck something because a fiber cleaver is precisely fabricated and is a sensitive tool. Moreover, a defective or worn cutter blade may also lead to an incorrectly cleaved fiber end.

3.4.2 Countermeasures

(1) Inspect a cleaved fiber end regularly (about once a week) to ensure good cleaving quality (using the display screen of an arc fusion splicer to view the cleaved fiber ends).
(2) Replace fiber cleaver blades (when incorrect cleaving is noticed or about once a month).
(3) Request the manufacturer to repair the fiber cleaver if no improvements result from the above countermeasures.

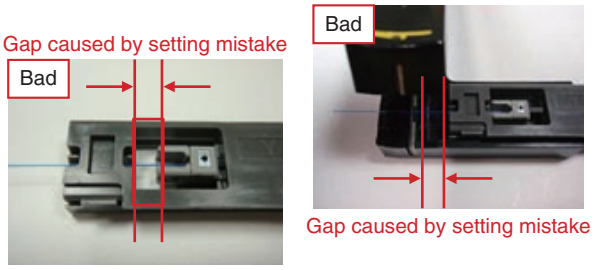

Fig. 6. Examples of incorrect optical fiber lengths.

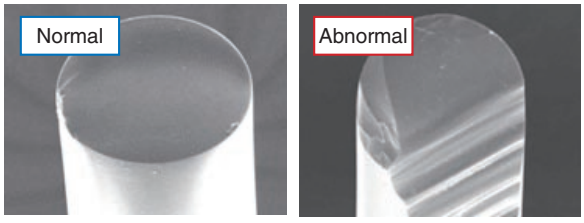

Fig. 7. Fiber ends (normal and abnormal).

3.5 Incorrect join to built-in optical fiber

3.5.1 Fault cases

Failures to correctly join an optical fiber to the built-in optical fiber in the mechanical splice part can lead to a large gap, which may result in an increase in loss.

3.5.2 Countermeasures

(1) Ensure that the wedge is correctly installed before inserting the bare optical fiber.
(2) Join the bare optical fiber to the built-in optical fiber and check that the fiber is sagging appropriately before releasing the wedge and fix the fiber.

4. Conclusion

This article introduced fault cases and countermeasures for field assembly connectors. All of the causes of faults can be eliminated by countermeasures such as correct use of tools and proper procedures. Looking forward, NTT EAST Technical Assistance and Support Center aims to accumulate and disseminate a variety of techniques and technologies for maintaining high-reliability network facilities.

Troubleshooting Tool for FLET'S TV

Abstract

NTT EAST Technical Assistance & Support Center has developed a tool called the RF Checker for troubleshooting problems in the homes of FLET'S TV customers (RF: radio frequency). It can be used to check video-signal levels and video quality using simple operations, which should make in-home troubleshooting much more efficient.

1. Introduction

FLET'S TV is a video broadcasting service that enables users to receive various types of broadcasts such as terrestrial digital broadcasts and BS (broadcast satellite) digital broadcasts through broadcast services offered by OptiCast Inc. via the FLET'S HIKARI optical fiber broadband service available from NTT EAST and NTT WEST. The FLET'S TV service model is shown in **Fig. 1**. First, the reception/delivery base receives video signals from satellites and terrestrial transmission towers via antennas and passes them to an optical transmitter after subjecting them to level adjustment, noise filtering, and other processes at head-end equipment. Next, the optical transmitter converts these electrical video signals to an optical signal, and transmits it. Finally, the NTT optical-fiber accommodation station amplifies and splits this optical signal at the video optical line terminals (V-OLTs), optically multiplexes it with an optical signal conveying FLET'S HIKARI communication signals from a Gigabit Ethernet OLT (GE-OLT) using an internal wavelength division multiplexing (WDM) splitter, and transmits them to a customer's home over a single strand of optical fiber. At the customer's home, an optical network unit (ONU) converts the WDM optical signals back to electrical video and communication signals. This ONU (GV-ONU) combines a V-ONU with a GE-ONU. The video signals arrive at television (TV) sets in the home via various types of wiring and devices such as coaxial cables, booster amplifiers, distributors, and branching filters.

† NTT EAST
Ota-ku, 144-0053 Japan

2. RF Checker

2.1 Development background

Since its launch in July 2008, FLET'S TV has increased its subscriber base steadily and further growth is expected in the future. Moreover, while maintenance of the coaxial-cable section in the customer's home was originally handled by the broadcasters, it was decided that NTT EAST and NTT WEST would take over maintenance for some users from March 2010 and April 2010, respectively. Therefore, NTT needed a means of performing prompt and accurate maintenance and troubleshooting in this coaxial-cable section. In response to this need, NTT EAST Technical Assistance & Support Center developed the RF Checker as a measurement tool that can be used by on-site technicians in the field to judge video quality even without specialized skills (RF: radio frequency). The RF Checker has the minimum necessary functions for measuring the quality of FLET'S TV in order to be an inexpensive and convenient handheld device that excels in operability and portability in the field.

2.2 Features

The features of the RF Checker are summarized below (**Fig. 2** and **Table 1**).

(1) Supports terrestrial digital, BS digital, and CS (communication satellite) digital (Sky PerfecTV! e2)
(2) Measures the following items:
· Level
· BER (pre): bit error rate before correction
· BER (post): bit error rate after correction
· CNR: carrier-to-noise ratio
(3) Evaluates measured values (level, BER, and CNR) on the basis of a threshold value and

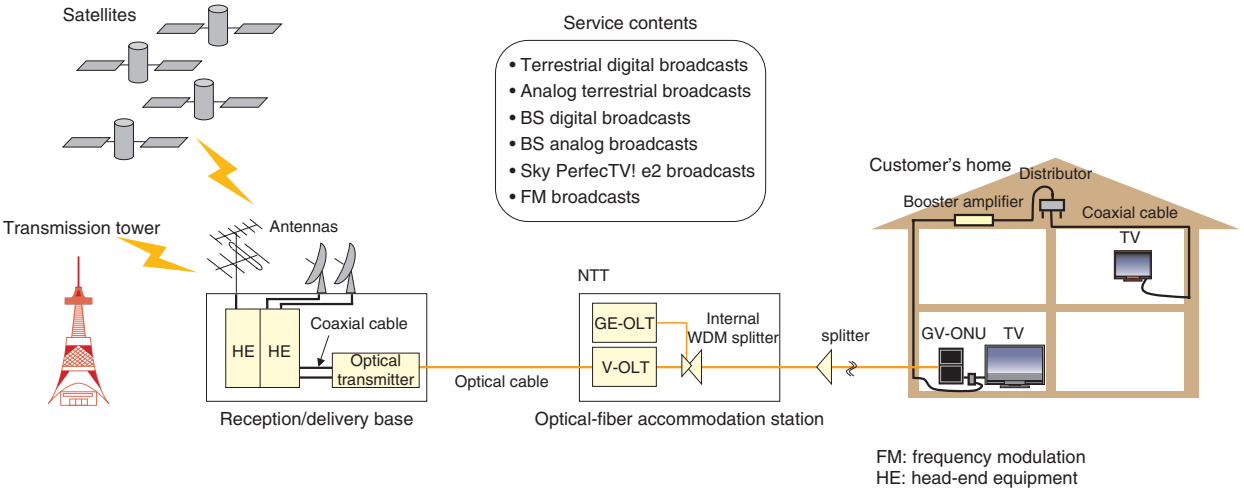

Fig. 1. FLET'S TV service model.

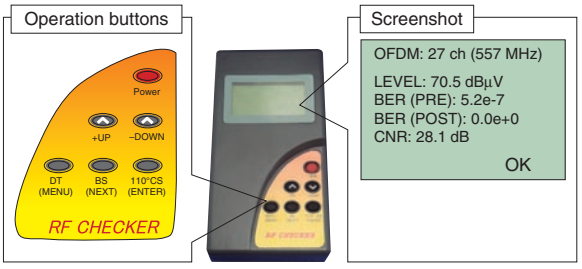

Power: On/off switch for power and backlight
+UP: Channel up
–DOWN: Channel down

OFDM: orthogonal frequency division multiplexing

DT: Select terrestrial digital broadcast
Channels 13–62 can be tested (channel allocation in Japan).
BS: Select BS digital broadcast
Channels 1–15 can be tested.
110° CS: Select 110° CS digital broadcast
Channels ND2–ND24 can be tested.
Other: Up to 100 measurement results can be stored in memory
Data can be transferred to a personal computer via USB.

Fig. 2. RF Checker.

Table 1. Specifications of the RF Checker.

Display method		Liquid crystal display (LCD) with backlight
Dimensions		86 mm (width) × 43 mm (depth) × 163 mm (height)
Measurement items		Level BER (pre) BER (post) CNR
Measurement range (level)		40 to 100 dBμV
Connection interface	RF terminal	75 Ω (F-type connector)
	USB	mini-USB connector
Power supply		Four type-3 (AA) dry-cell batteries
Accessories		Protective case, dedicated USB cable, user manual * Dry-cell batteries and coaxial cables for measurements are not included and need to be obtained separately.

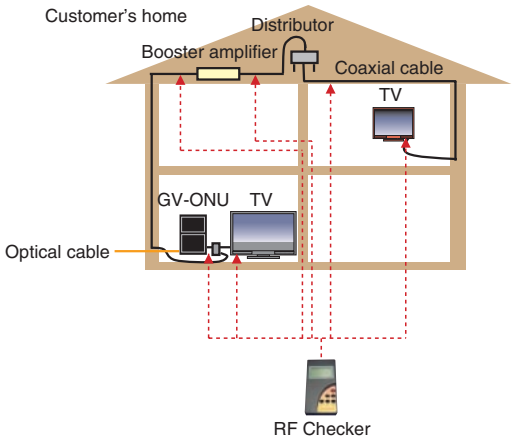

Fig. 3. RF Checker usage points.

displays OK or NG (okay or no good). Threshold values may be set as desired.

(4) Saves measurement results in internal memory (maximum 100 items)

(5) Transfers saved data to a personal computer via a USB (universal serial bus) connection

2.3 Use

The RF Checker is operated as follows. It is turned on by briefly holding down the power-supply button and then connected to a coaxial cable (F-type connector) inside the customer's home. Next, the button for the type of broadcast (terrestrial digital, BS, or CS) to be measured is pressed and a channel is selected by pressing the +UP or –DOWN button to begin automatic measurement. Results are displayed within a few seconds all together on one screen. They consist of level, BER (pre), BER (post), and CNR as well as OK or NG indicating whether those results are acceptable according to the threshold values.

An on-site technician using the RF Checker during maintenance work can easily perform troubleshooting by measuring video quality at the GV-ONU video output terminal, at the coaxial terminal in each room in the coaxial-cable section, at the input/output terminals of the booster amplifier and distributors, or at the coaxial connector nearest to a TV.

Actual troubleshooting begins from the TV side when video problems occur in only one TV set and from the ONU side when video problems occur in more than one TV set. Using the RF Checker, the technician can observe the display of OK or NG at multiple measurement points (or the display of "× under" instead of OK/NG in the case of a low level) and can conclude that a problem exists at the point where the display of OK/NG or "× under" changes. RF Checker usage points are shown in **Fig. 3**.

3. Concluding remarks

The RF Checker was released in February 2010. As of the end of March 2011, about 590 units are in use by the maintenance departments of NTT EAST and WEST and partner companies. Looking forward, we expect the number of problem incidents to increase as the use of FLET'S TV expands, but we also expect the use of the RF Checker as a troubleshooting tool inside customer homes to make repairs more efficient and raise the level of maintenance.

Corrosion Diagnosis Equipment for Inspecting Suspension Cables

Abstract

NTT has developed equipment for diagnosing corrosion in aerial suspension cables as an inspection tool. Although suspension cables use corrosion-resistant strands of steel wire having high anti-corrosion properties, cables in coastal areas can still suffer from localized corrosion inside the nozzle section of a terminal box. This diagnostic equipment can analyze such hidden corrosion nondestructively.

1. Introduction

Aerial metallic cables and optical fiber cables are supported by a steel suspension cable running between utility poles. Modern suspension cables are made of highly corrosion-resistant strands of steel wire having both high anti-corrosion and anti-fatigue properties. In coastal areas, however, localized corrosion can still occur under the sealing tape in the nozzle section of a terminal box, as shown in **Fig. 1**. Such localized corrosion may often exist despite the absence of corrosion on the outside of the nozzle section, so a conventional visual inspection will fail to detect any corrosion at all. For a full inspection, it is therefore necessary to dismantle the nozzle, so the inspection is long and costly. NTT therefore felt the need for equipment that could diagnose suspension-cable corrosion inside the nozzle section nondestructively.

2. Inspection tool

The diagnostic equipment consists of a main unit, ultrasonic sensor, fixture, and cable (**Fig. 2**). Ultrasonic pulses are transmitted inside the suspension cable from the ultrasonic sensor, as shown in **Fig. 3**. At local corrosion sites, the ultrasonic waves are reflected back to the sensor, where they are detected.

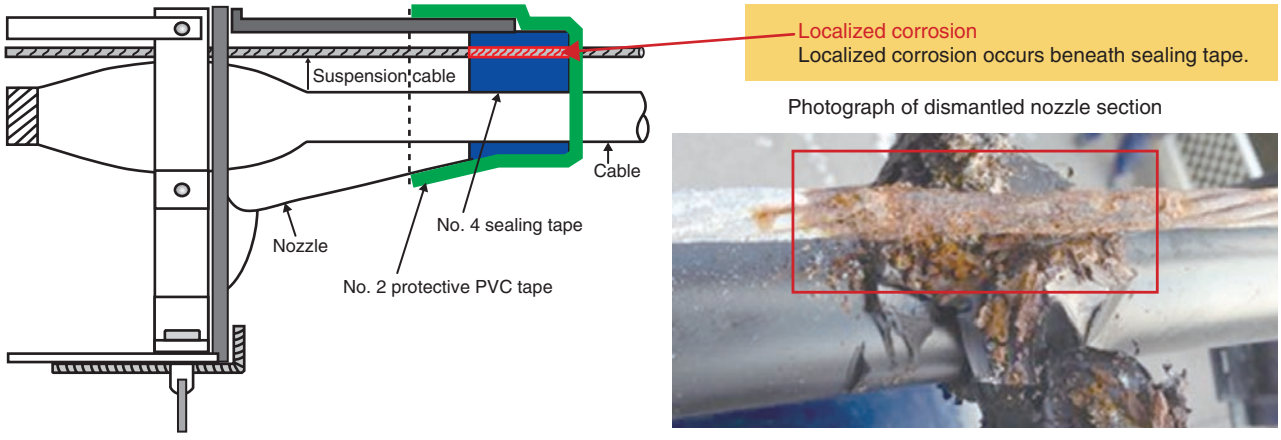

Fig. 1. Example of localized corrosion in a suspension cable inside the nozzle section of a terminal box.

† NTT EAST
Ota-ku, 144-0053 Japan

The waveforms of the reflected waves enable the presence and extent of corrosion to be determined.

For better positioning accuracy and reproducibility of ultrasonic sensor results in corrosion inspections, the sensor is attached to the suspension cable using a fixture so that it emits ultrasonic waves into two wire strands at a time. Since the suspension cable consists of six outer wire strands surrounding a seventh central strand, the sensor must be put at three positions to inspect the six outer wire strands. In addition, one reference measurement is also performed to ensure that the surface conditions of the suspension cable do not affect the results, so a total of four measurements must be taken.

A polymer sheet is inserted between the ultrasonic sensor and the suspension cable as a contact medium. Although it is common to use a gel such as glycerin with ultrasonic sensors, if the gel were to get among the cable strands, it could itself act as a source of corrosion, so for this reason and for better operability in the field, we decided to use a polymer sheet applicable to suspension cable diagnosis.

An example of the waveform of waves reflected from a corroded section is shown in **Fig. 4**. This waveform is determined by the degree of corrosion and the distance of the corrosion site from the ultrasonic sensor. It is analyzed in the background on the diagnostic equipment and only the result of the corrosion level is displayed on the screen in an easy-to-understand manner.

3. Inspection method

The inspection method is shown in **Fig. 5**. A maintenance worker inspects a suspension cable from an aerial work platform positioned next to the terminal box. The inspection procedure is presented to the maintenance worker via figures and photographs displayed on the screen of the main unit one step at a time. Referring to these instructions, the maintenance worker attaches the ultrasonic sensor to the suspension cable using the fixture and proceeds to take measurements. If six wire strands are to be measured, for example, the instructions will use figures or images to show how the ultrasonic sensor should be slid along the suspension cable to measure three strand pairs. The worker will also be prompted to visually check for rust on the outside of the nozzle section emerging from the nozzle's interior because corrosion progressing inside the nozzle section eventually appears as red rust outside the nozzle section. In short, the visual detection of rust is a sure sign of internal corrosion and evidence that the suspension cable needs renovation as soon as possible. Finally, the diagnostic equipment displays the diagnosis

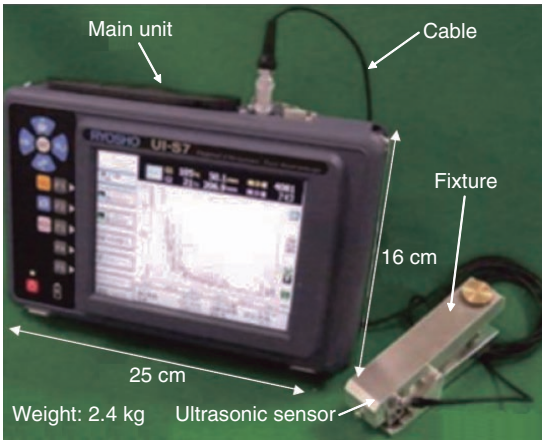

Fig. 2. Appearance of diagnostic equipment.

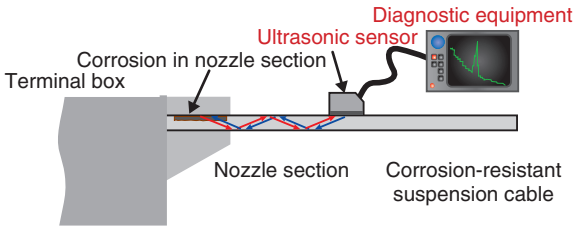

Fig. 3. Principle of diagnosis by ultrasonic waves.

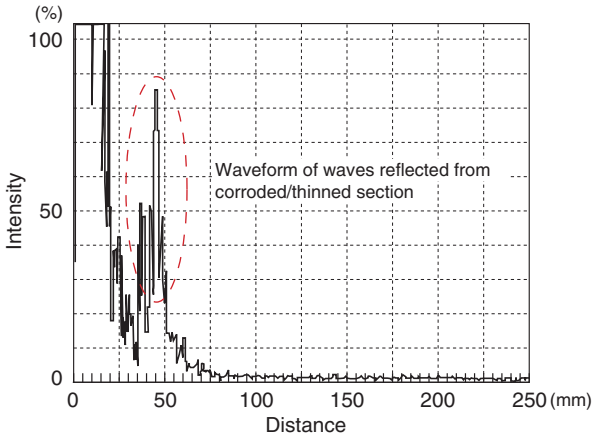

Fig. 4. Waveform of waves reflected from corroded section.

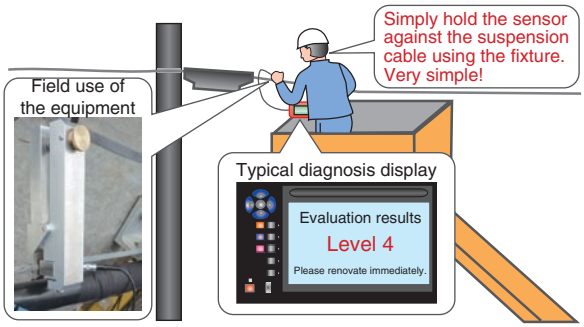

Fig. 5. Example of suspension-cable corrosion diagnosis in the field.

results. As shown in the example in Fig. 5, these results simply indicate the level of corrosion and the need for renovation.

4. Conclusion

It has been more than twenty years since corrosion-resistant suspension cables were first introduced, but because they are becoming increasingly used in coastal areas as well, we can expect the need for localized-corrosion inspections to grow. The suspension-cable corrosion diagnostic equipment can significantly reduce the inspection time and enable a large number of inspections of facilities by eliminating the need to dismantle nozzles of terminal boxes. As a result, effective maintenance becomes possible.

Measurement-based Quantum Computation and the Fault-tolerant System

Yuuki Tokunaga†

Abstract

Quantum computation provides us with a new form of information processing that surpasses current computer technology. In a new model of quantum computation, measurement-based quantum computation, the computation proceeds via simple measurements on previously prepared quantum entangled states. This model has attracted attention for its good potential for realizing quantum computers. This article reviews the basic concepts of measurement-based quantum computation and the elegant fault-tolerant system called topological one-way quantum computation.

1. Introduction

The principle of current information processing performed by computers and networks is based on the physics of classical electromagnetic dynamics. Information processing technology based on this principle has blossomed in the 20th century as electronics. Meanwhile, a new principle of physics, quantum dynamics, was discovered in the early 20th century for describing the world on the small scale: the scale of the smallest particles and sub-particles. After a while, in the late 20th century, a new principle of information processing based on quantum physics started to be considered. As a result, groundbreaking information processing was found to be possible, such as efficient computation of prime factorization, unconditionally secure communication, and teleportation of quantum information [1]. However, quantum information processing is not easy to realize because the quantum states are difficult to manipulate precisely and are not stable for a long time; i.e., they easily decohere. A lot of study has been going on to achieve the breakthrough needed to realize quantum information processing.

† NTT Information Sharing Platform Laboratories
Musashino-shi, 180-8585 Japan

In this article, I review a new computational model for achieving quantum computers called measurement-based quantum computation. Section 2 describes the basic concepts and advantages of measurement-based quantum computation and compares it with the conventional computational model: the circuit model. Section 3 describes an important new fault-tolerant system for quantum computation, topological quantum computing, that can be performed on the basis of the measurement-based quantum computation model in an elegant way. Section 4 describes research on measurement-based quantum computation at NTT laboratories. Section 5 mentions the outlook for future research.

2. Measurement-based quantum computation

From the beginning of the study of quantum computation in around 1990, the realization of quantum computers has been considered on the basis of a standard computational model: the circuit model (**Fig. 1**). It has a few basic gates such as single-qubit (quantum bit) rotation gates and an important two-qubit interaction gate: the controlled-NOT gate. The input state to the combination of the basic gates achieves universal quantum computation. However, one of the main difficulties in realizing quantum computers is how to

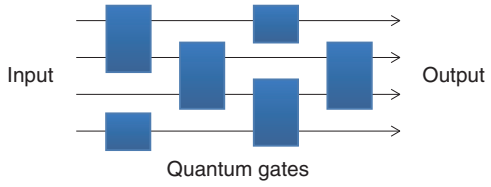

Fig. 1. Circuit model.

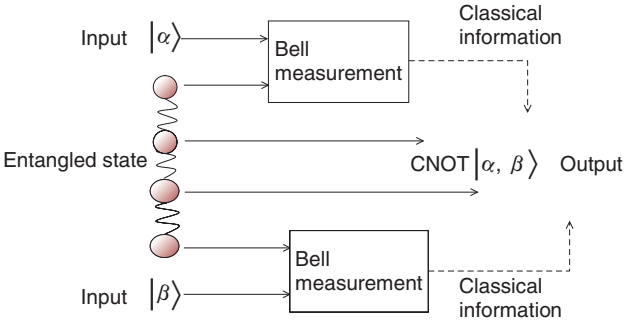

Fig. 2. Teleportation-based gate.

make the controlled-NOT gate. It is not easy to obtain an appropriate interaction between particles such as atoms or photons. To date, many experiments toward the controlled-NOT gate have been performed.

A whole new paradigm for quantum computers started in around 2000. Researchers began to reconsider the computational model in order to utilize the unique features of quantum physics. They thought that there might be a completely different computational model for quantum computers than the one based on the idea of the classical circuit model because the physics is completely different from classical physics. The great feature of quantum states is the existence of *entanglement*. A breakthrough idea for utilizing entanglement for quantum computers was described by Gottesman and Chuang [2]. They proposed a new model of quantum gates that operate by means of quantum teleportation. Quantum teleportation is a quantum information transmission process that consumes the quantum entanglement in compensation for sending quantum information. We can obtain the output of a controlled-NOT gate by operating quantum teleportation using a special entangled state **(Fig. 2)**. The entangled state can be regarded as a computational resource for the quantum gate.

A more sophisticated computational model based

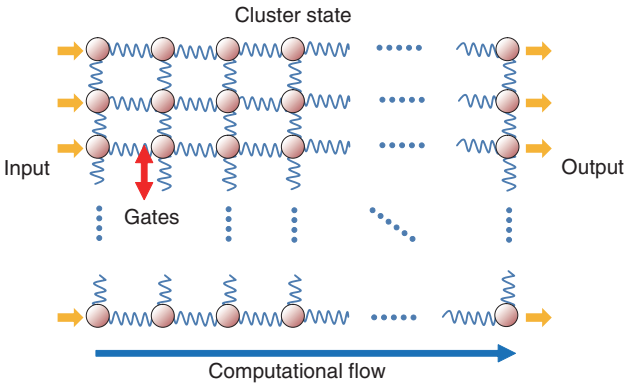

Fig. 3. One-way quantum computation.

on the teleportation-based gate is *one-way quantum computation* **(Fig. 3)** [3]. First, a special entangled state, called a cluster state, is prepared beforehand. After that, one only has to perform single-qubit measurement on the cluster state and one can then perform universal quantum computation, in which the entangled cluster state plays the roles of quantum gates and the information flow. The cluster state is a specific entangled state and it can be prepared before computation is started. The entanglement preparation is easier than computation because the target state is known beforehand. Actually, we can even utilize a non-deterministic gate having a low success probability in order to generate the entangled resource [4], [5]. Once the computational resource of the entanglement has been prepared, one only needs to perform single-qubit measurements; this is a very simple task compared with two-qubit interaction gates, so the new computational model significantly decreases the difficulty of realizing quantum computers.

3. Fault-tolerant topological quantum computation

We also need to protect the quantum computing from decoherence and from the effects of several kinds of noise. Fortunately, error correction codes are available for quantum computing and we can perform fault-tolerant quantum computing by applying an error correction procedure appropriately during computation. A well-known fault-tolerant system based on the circuit model used a quantum linear code and concatenated codes **(Fig. 4)** [6], [7]. A standard quantum linear code encodes a single qubit into several qubits. It can tolerate a single bit-flip and phase-flip

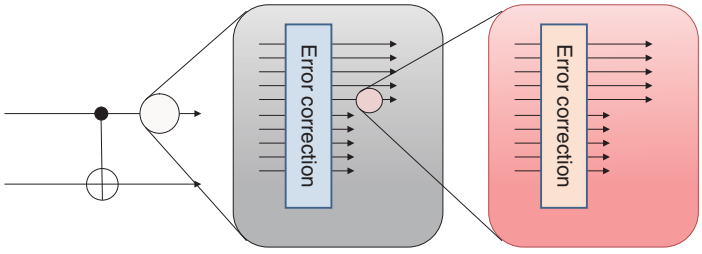

Fig. 4. Concatenated code.

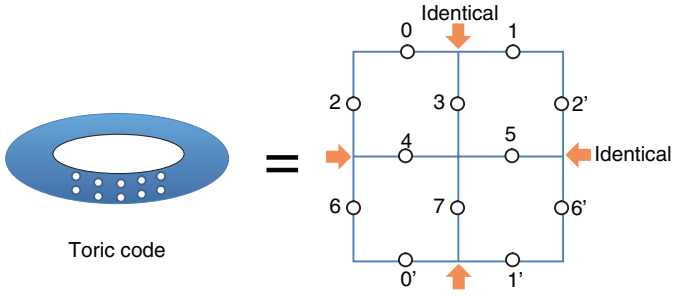

Fig. 5. Topological code.

error, but if more than one error occurs in the encoded state, then the error correction does not work well. Concatenated coding solves this problem. It recursively uses the linear code as shown in Fig. 4. It provides greater error tolerance if the error rate per basic computational unit is less than a certain threshold. Reliable quantum computing can be executed by using code concatenation of sufficient depth with the error rate below the threshold. The threshold of fault-tolerant systems based on the circuit model is known to be around 1% [7]. However, it is assumed here that any quantum gate can be achieved between widely separated particles, but the interaction between particles normally becomes weaker with increasing distance between particles. Thus, this assumption is unnatural from the physical viewpoint. Though we can rewrite the quantum gate between spatially separate particles into combinations of quantum gates between nearest-neighbor sites, the number of consumed gates becomes larger in that case and the threshold of the fault-tolerant system becomes significantly small.

Considering the shortage of concatenated codes for fault-tolerant systems, elegant quantum codes treating physical nearest-neighbor interactions were proposed [8]. They are called topological codes or surface codes; the name originates from the topological nature of the code. The important point is that a topological code uses only nearest-neighbor interactions. This is a realistic scenario compared with the circuit model. An example of a two-dimensional (2D) topological code, toric code, is shown in **Fig. 5**. The qubits are on the edges of the 2D lattice and entangled as a topological code state. In toric code, the qubits on the endpoints of the 2D lattice are identical to those at the other sides; that is, the 2D lattice is on the surface of a torus, which gives us the degrees of freedom for encoding logical qubits. The entangled code state can be prepared through the use of only nearest-neighbor interactions and the error-checking operations can also be operated by nearest-neighbor interactions and single-site measurements. The encoding size can be enlarged by expanding the lattice size. Toric code can also be rewritten on a square lattice with boundaries by constructing the equivalent for the hole of the torus and introducing the same topology. That makes it easier to prepare multiple logical qubits. Topological fault-tolerant quantum computation is known to be possible in a 2D square lattice with nearest-neighbor interactions during computation, where the obtained noise threshold is 0.75% [9]. Moreover, a special form of 3D cluster state becomes a resource

of fault-tolerant topological one-way quantum computation with noise threshold of 0.11% [10]. In this case, we can perform fault-tolerant quantum computing with only single-qubit measurements after preparing the 3D cluster states. The thresholds can be improved by devising better encoding and decoding methods [11], [12]. Recently, the important realistic case of errors with a high loss rate [13] and of nondeterministic entangling gates [14], [15] have also been investigated.

4. NTT research on measurement-based quantum computation

Here, I briefly describe research on measurement-based quantum computation at NTT Laboratories. In 2008, my colleagues and I experimentally demonstrated a simple scheme for generating a four-photon entangled cluster state and basic operations for one-way quantum computing using the produced state [16]. We showed that the output state fidelities surpass classical bounds, which indicates that the entanglement in the produced state essentially contributes to the quantum operation. However, the obtained fidelities have not been sufficiently high for fault-tolerant quantum computation. In order to perform quantum computing fault-tolerantly, we must improve the gate fidelities experimentally. At the same time, it is important to improve the theory of fault-tolerant quantum computing so that we can utilize realistic imperfect devices. For example, in linear optics, two-qubit gates are intrinsically nondeterministic owing to the linearity of the interaction [4], [17]. In other systems, it is also often the case that a large amount of error such as photon loss and detector inefficiency can be detected in heralded ways, and one can postselect successful events [16], [18]. In 2010, we proposed a scalable way to construct a 3D cluster state for fault-tolerant topological one-way quantum computation using such nondeterministic two-qubit gates with a low success probability [14]. We showed that fault-tolerant topological one-way quantum computation can be performed with a two-qubit gate success probability of less than 1/2 provided that the unheralded error probability of the two-qubit gate is sufficiently small. This work showed for the first time that realistic imperfect nondeterministic gates with a success probability of less than 1/2 can also be utilized for fault-tolerant quantum computing. The other issue in measurement-based quantum computation, reducing the computational resources, is discussed in the second Regular Article [19], which treats a different model of measurement-based quantum computation.

5. Future outlook

Having reviewed the concepts and favorable features of measurement-based quantum computation and the fault-tolerant system, I would like to mention the outlook for future research. On the theoretical side, an important task is to find a more realistic physical model for realizing measurement-based quantum computation. There have been studies for finding Hamiltonians whose ground states are universal resources for measurement-based quantum computation [20], [21]. On the experimental side, some demonstrations of measurement-based quantum computation have been performed [16], [18], [22]. However, a lot of problems remain to be overcome. The most important one is how to obtain scalability in quantum computers. For optical quantum computation, a new high-efficiency single-photon source is necessary [23]. A promising candidate for preparing a large entangled resource for measurement-based quantum computation is ultracold atomic gas in an optical lattice [24]. The important issue for future work on the optical lattice is single-site addressing [25], [26]. Another important candidate is the use of solid-state artificial atoms such as quantum dots or dopants in solids for stationary qubits and the use of atom-photon interactions with cavity quantum electrodynamics for the quantum gates [27]. In conclusion, measurement-based quantum computation provides us with great features toward realizing quantum computers and has high potential for both theoretical and experimental research in the future.

References

[1] M. A. Nielsen and I. L. Chuang, "Quantum Computation and Quantum Information," Cambridge University Press, 2000.

[2] D. Gottesman and I. Chuang, "Demonstrating the Viability of Universal Quantum Computation Using Teleportation and Single-qubit Operations," Nature, Vol. 402, pp. 390–393, 1999.

[3] R. Raussendorf and H. J. Briegel, "A One-way Quantum Computer," Phys. Rev. Lett., Vol. 86, No. 22, pp. 5188–5191, 2001.

[4] D. E. Browne and T. Rudolph, "Resource-efficient Linear Optical Quantum Computation," Phys. Rev. Lett., Vol. 95, No. 1, p. 010501, 2005.

[5] L.-M. Duan and R. Raussendorf, "Efficient Quantum Computation with Probabilistic Quantum Gates," Phys. Rev. Lett., Vol. 95, No. 8, p. 080503, 2005.

[6] D. Aharonov and M. Ben-Or, "Fault-tolerant Quantum Computation with Constant Error Rate," SIAM Journal on Computing, Vol. 38, No. 4, pp. 1207–1282, 2008.

[7] E. Knill, "Quantum Computing with Realistically Noisy Devices," Nature, Vol. 434, pp. 39–44, 2005.

[8] A. Y. Kitaev, "Fault-tolerant Quantum Computation by Anyons," Annals of Physics, Vol. 303, No. 1, pp. 2–30, 1997.

[9] R. Raussendorf and J. Harrington, "Fault Tolerant Quantum Computation with High Threshold in Two Dimensions," Phys. Rev. Lett., Vol. 98, No. 19, p. 190504, 2007.
[10] R. Raussendorf, J. Harrington, and K. Goyal, "A Fault-tolerant One-way Quantum Computer," Annals of Physics, Vol. 321, No. 9, pp. 2242–2270, 2005.
[11] R. Raussendorf, J. Harrington, and K. Goyal, "Topological Fault-tolerance in Cluster State Quantum Computation," New J. Phys., Vol. 9, 199, 2007.
[12] D. Wang, A. Fowler, and L. Hollenberg, "Surface Code Quantum Computing with Error Rates over 1%," Phys. Rev. A, Vol. 83, No. 2, 020302(R), 2011.
[13] S. Barrett and T. Stace, "Fault Tolerant Quantum Computation with Very High Threshold for Loss Errors," Phys. Rev. Lett., Vol. 105, No. 20, 200502, 2010.
[14] K. Fujii and Y. Tokunaga, "Fault-tolerant Topological One-way Quantum Computation with Probabilistic Two-qubit Gates," Phys. Rev. Lett., Vol. 105, No. 25, 250503, 2010.
[15] Y. Li, S. Barrett, T. Stace, and S. Benjamin, "Fault Tolerant Quantum Computation with Nondeterministic Gates," Phys. Rev. Lett., Vol. 105, No. 25, 250502, 2010.
[16] Y. Tokunaga, S. Kuwashiro, T. Yamamoto, M. Koashi, and N. Imoto, "Generation of High-fidelity Four-photon Cluster State and Quantum-domain Demonstration of One-way Quantum Computing," Phys. Rev. Lett., Vol. 100, No. 21, 210501, 2008.
[17] E. Knill, R. Laflamme, and G. Milburn, "A Scheme for Efficient Quantum Computation with Linear Optics," Nature, Vol. 409, pp. 46–52, 2001.
[18] P. Walther, K. J. Resch, T. Rudolph, E. Schenck, H. Weinfurter, V. Vedral, M. Aspelmeyer, and A. Zeilinger, "Experimental One-way Quantum Computing," Nature, Vol. 434, , pp. 169–176, 2005.
[19] Y. Takahashi, "Reducing the Resources in Measurement-only Quantum Computation," NTT Technical Review, Vol. 9, No. 7, 2011. https://www.ntt-review.jp/archive/ntttechnical.php?contents=ntr201107ra2.html
[20] T.-C. Wei, I. Affleck, and R. Raussendorf, "Affleck-Kennedy-Lieb-Tasaki State on a Honeycomb Lattice is a Universal Quantum Computational Resource," Phys. Rev. Lett., Vol. 106, No. 7, 070501, 2011.
[21] M. Van den Nest, A. Miyake, W. Dür, and H. J. Briegel, "Universal Resources for Measurement-based Quantum Computation," Phys. Rev. Lett., Vol. 97, No. 15, 150504, 2006.
[22] W.-B. Gao, A. M. Goebel, C.-Y. Lu, H.-N. Dai, C. Wagenknecht, Q. Zhang, B. Zhao, C.-Z. Peng, Z.-B. Chen, Y.-A. Chen, and J.-W. Pan, "Teleportation-based Realization of an Optical Quantum Two-qubit Entangling Gate," Proc. of the Natl. Acad. Sci. USA, Vol. 107, pp. 20869–20874, 2010.
[23] J. L. O'Brien, "Optical Quantum Computing," Science, Vol. 318, No. 5856, pp. 1567–1570, 2008.
[24] I. Bloch, "Quantum Coherence and Entanglement with Ultracold Atoms in Optical Lattices," Nature, Vol. 453, pp. 1016–1022, 2008.
[25] A. Daley, M. Boyd, J. Ye, and P. Zoller, "Quantum Computing with Alkaline-Earth-Metal Atoms," Phys. Rev. Lett., Vol. 101, No. 17, 170504, 2008.
[26] K. Shibata, S. Kato, A. Yamaguchi, S. Uetake, and Y. Takahashi, "A Scalable Quantum Computer with Ultranarrow Optical Transition of Ultracold Neutral Atoms in an Optical Lattice," Appl. Phys. B, Vol. 97, No. 2, pp. 753–758, 2009.
[27] T. D. Ladd, F. Jelezko, R. Laflamme, Y. Nakamura, C. Monroe, and J. L. O'Brien, "Quantum Computers," Nature, Vol. 464, pp. 45–53, 2010.

Yuuki Tokunaga
Research Scientist, Distinguished Researcher, Okamoto Research Laboratory, NTT Information Sharing Platform Laboratories.

He received the bachelor's degree in integrated human studies in mathematical science from Kyoto University in 1999, the M.S. degree in information science from the University of Tokyo in 2001, and the Ph.D. degree in materials physics from Osaka University in 2007. He joined NTT Information Sharing Platform Laboratories in 2001. Since then, he has been engaged in research on quantum information science, especially on optical quantum information processing. He received the 2008 Inoue Research Award for Young Scientists and the NTT Information Sharing Laboratory Group Director's Award in 2008 and 2010. He is a member of the Physical Society of Japan.

Reducing the Resources in Measurement-only Quantum Computation

Yasuhiro Takahashi†

Abstract

This article describes a recent result concerning the construction of a small set of projective measurements required for implementing universal quantum computation, that is, for implementing an arbitrary unitary operation. Projective measurements are used as the main resources for implementing an arbitrary unitary operation in the measurement-only quantum computation model in contrast to conventional models. Resource minimization is important not only for realizing a quantum computer based on the measurement-only quantum computation model, but also for understanding the computational power of projective measurements.

1. Introduction

Quantum computers are expected to enable high-speed computing and many researchers have made numerous attempts to realize them. However, a practical quantum computer has not yet been made. Most of the attempts are based on the standard model of quantum computation, which is called the quantum circuit model or gate-based quantum computation [1], [2]. The main resources for universal quantum computation, that is, for implementing an arbitrary unitary operation, are unitary gates that perform one-qubit and two-qubit unitary operations. A computation proceeds by applying unitary gates to an input state to transform it into an appropriate output one. Projective measurements of the output state give us the final output of the computation, which is classical information.

In 2003, on the basis of an idea described by Gottesman and Chuang [3], Nielsen proposed a model of quantum computation [4] strikingly different from the standard model. This model is called teleportation-based or measurement-only quantum computation. The main resources required for universality are only projective measurements. A computation proceeds by performing projective measurements on an input state to transform it into an appropriate output one. Projective measurements on the output state give us the final output of the computation. This model has recently attracted attention since it allows us to make completely new attempts to realize quantum computers. An important problem is to minimize the resources required for universality. From the practical standpoint, solutions to this problem will contribute to the performance of unitary operations on a quantum computer since it will be able to use only a limited amount of resources. On the theoretical side, they will contribute to our understanding of the computational power of projective measurements.

Let us consider the problem of minimizing the resources required for universality in measurement-only quantum computation. There have been many studies in this direction [5]–[8]. The best known result is that a set consisting of one two-qubit projective measurement and infinitely many kinds of one-qubit projective measurements with one ancillary qubit is sufficient for universal quantum computation [8]. Since it is impossible to decrease the number of two-qubit projective measurements and the number of ancillary qubits, we shall focus on one-qubit projective measurements. Thus, our problem is restated

† NTT Communication Science Laboratories
Atsugi-shi, 243-0198 Japan

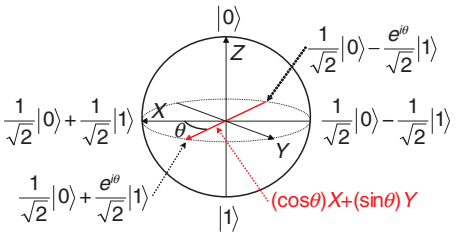

Fig. 1. Unit three-dimensional sphere representing one-qubit states.

as the problem of constructing a small set of one-qubit projective measurements such that the set with one two-qubit projective measurement and one ancillary qubit is sufficient for universal quantum computation.

The state of a qubit corresponds to a point on the unit three-dimensional sphere (**Fig. 1**) [1] and a one-qubit projective measurement corresponds to an axis, which is a line through the origin of the sphere. There are two points of intersection between an axis and the sphere. A one-qubit projective measurement probabilistically projects a one-qubit state into one of the two states corresponding to the two intersection points on the sphere. The best known result requires the set consisting of one-qubit projective measurements corresponding to all the axes of the sphere's X-Y plane and the Z axis [8]. Until recently, it was not known whether a smaller set of one-qubit projective measurements could be constructed for universal quantum computation.

In this article, I describe my recent result that this can be done [9]. Specifically, I show that the set consisting of one-qubit projective measurements corresponding to all the axes of the sphere's X-Y plane (with one two-qubit projective measurement and one ancillary qubit) is sufficient for universal quantum computation. In other words, I show that the one-qubit projective measurement corresponding to the Z axis can be removed from the best known set. A key finding is that the one-qubit projective measurement corresponding to the Y axis can often be used in place of the one-qubit projective measurements corresponding to the X and Z axes. In particular, a key ingredient of my procedure for implementing an arbitrary one-qubit unitary operation is a simplified version of quantum teleportation (called state transfer) based on the one-qubit projective measurement corresponding to the Y axis.

2. Measurement-only quantum computation

2.1 Quantum states and projective measurements

As described above, the state of a qubit corresponds to a point on the unit three-dimensional sphere (Fig. 1). The two points of intersection of the Z axis and the sphere are represented by $|0\rangle$ and $|1\rangle$. The other points on the sphere correspond to superposition states of $|0\rangle$ and $|1\rangle$. For example, the two points of intersection of the X axis and the sphere are $\frac{1}{\sqrt{2}}|0\rangle + \frac{1}{\sqrt{2}}|1\rangle$ and $\frac{1}{\sqrt{2}}|0\rangle - \frac{1}{\sqrt{2}}|1\rangle$. Moreover, the two points of intersection of the Y axis and the sphere are $\frac{1}{\sqrt{2}}|0\rangle + \frac{i}{\sqrt{2}}|1\rangle$ and $\frac{1}{\sqrt{2}}|0\rangle - \frac{i}{\sqrt{2}}|1\rangle$. In general, a one-qubit state is represented as $\alpha|0\rangle + \beta|1\rangle$, where α and β are complex numbers such that $|\alpha|^2 + |\beta|^2 = 1$.

A one-qubit projective measurement corresponds to an axis L, which is a line through the sphere's origin. It probabilistically projects a one-qubit state into one of the two states corresponding to the two points of intersection of L and the sphere. The probability depends on the state being measured. The measurement gives us the classical outcome (1 or -1) representing which of the two states the original state is projected into by the measurement. We call such a measurement an L-measurement. For example, the Z-measurement of a qubit in state $\alpha|0\rangle + \beta|1\rangle$ projects the state into $|0\rangle$ with probability $|\alpha|^2$ and into $|1\rangle$ with probability $|\beta|^2$. In general, an axis of the sphere's X-Y plane is represented by $(\cos\theta)X+(\sin\theta)Y$ for some real number $\theta \in [0,2\pi)$. It corresponds to the one-qubit projective measurement that probabilistically projects a one-qubit state into one of the two states $\frac{1}{\sqrt{2}}|0\rangle + \frac{e^{i\theta}}{\sqrt{2}}|1\rangle$ and $\frac{1}{\sqrt{2}}|0\rangle - \frac{e^{i\theta}}{\sqrt{2}}|1\rangle$.

2.2 Measurement-based quantum circuits

A computational procedure in measurement-only quantum computation can be represented by a measurement-based quantum circuit (very similar to the standard quantum circuit [2]). It consists of wires and measurement gates that correspond to qubits and projective measurements, respectively. In a circuit diagram, a wire is represented by a horizontal line and a measurement gate is represented by the axis symbol corresponding to the projective measurement on the wires on which it is performed. Information flows through the circuit from left to right.

As an example, consider the measurement-based

quantum circuit depicted in **Fig. 2**. It represents the following procedure, where the initial state of qubit 1 is $|\varphi\rangle$ and that of qubit 2 is an arbitrary one-qubit state.

(1) Perform the X-measurement on qubit 2.
(2) Perform the $Z\otimes Z$-measurement on qubits 1 and 2.
(3) Perform the X-measurement on qubit 1.

I do not give details of the $Z\otimes Z$-measurement here, but in general it generates a two-qubit state that cannot be represented as a product form (called entangled state).

The procedure outputs the state $\sigma|\varphi\rangle$ on qubit 2 for some unitary operation σ, which is in a special class of unitary operations called Pauli operations. An important point is that σ is determined by the classical outcomes of the projective measurements in the procedure, and the inverse of σ can be performed by the Y-measurements (and one two-qubit projective measurement and one ancillary qubit). Thus, σ can be easily removed and thus ignored. That is, the procedure transfers an arbitrary one-qubit state from qubit 1 to qubit 2 (up to Pauli operations) and thus is called state transfer [6]. It can be regarded as a simplified version of quantum teleportation.

As shown in [6], state transfer is a key ingredient of a procedure for implementing an arbitrary one-qubit unitary operation. More precisely, a procedure for implementing such an operation (up to Pauli operations) can be obtained by replacing the projective measurements in the state transfer with ones that depend on the desired operation. For example, a procedure for implementing a Hadamard operation H can be obtained by replacing the first measurement with the Z-measurement and the second measurement with the $Z\otimes X$-measurement, where H is the one-qubit unitary operation that maps $|0\rangle$ and $|1\rangle$ to

$\frac{1}{\sqrt{2}}|0\rangle + \frac{1}{\sqrt{2}}|1\rangle$ and $\frac{1}{\sqrt{2}}|0\rangle - \frac{1}{\sqrt{2}}|1\rangle$, respectively.

3. Universal set of projective measurements

I will show that the set consisting of the one-qubit projective measurement corresponding to the axis $(\cos\theta)X+(\sin\theta)Y$ for any $\theta\in[0,2\pi)$ (with one two-qubit projective measurement and one ancillary qubit) is sufficient for universal quantum computation. To do this, I will show that an arbitrary unitary operation can be implemented using only the above projective measurements. Since an arbitrary unitary operation can be implemented by combining one-qubit unitary operations with a two-qubit unitary operation [1], it suffices to show how to implement these operations.

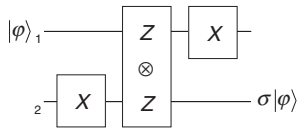

Fig. 2. Measurement-based quantum circuit proposed for state transfer [6].

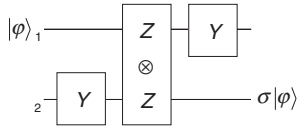

Fig. 3. State transfer based on Y-measurements.

3.1 New state transfer

A key ingredient of my procedure for implementing an arbitrary one-qubit unitary operation is a new state transfer based on the Y-measurements. Consider the following procedure (**Fig. 3**), where the initial state of qubit 1 is $|\varphi\rangle$ and that of qubit 2 is an arbitrary one-qubit state.

(1) Perform the Y-measurement on qubit 2.
(2) Perform the $Z\otimes Z$-measurement on qubits 1 and 2.
(3) Perform the Y-measurement on qubit 1.

The procedure can be shown to be a state transfer, which transfers the input state from qubit 1 to qubit 2. It is obtained by replacing the X-measurements in the previous state transfer with the Y-measurements. That is, this is an example of the case where the Y-measurements can be used in place of the X-measurements.

3.2 Implementations of one-qubit and two-qubit unitary operations

I will deal with one-qubit unitary operations first. I can show that, by replacing the $Z\otimes Z$-measurement in the new state transfer with the $Z\otimes X$-measurement, the resulting procedure is the one for implementing H. An important point is that it uses only Y-measurements, though the previous procedure for implementing H uses the X- and Z-measurements as described above. This can be considered an example of the case where the Y-measurements can be used in place of the

X- and Z-measurements. That is, the new state transfer provides an H implementation procedure that requires only a small set of one-qubit projective measurements. By generalizing the method for transforming the new state transfer into an H implementation procedure, I can obtain a procedure for implementing an arbitrary one-qubit unitary operation (up to Pauli operations). Moreover, I can show that it requires only the one-qubit projective measurement corresponding to the axis $(\cos\theta)X+(\sin\theta)Y$ for any $\theta\in[0,2\pi)$.

As a two-qubit unitary operation, it suffices to deal with the controlled-Z operation ΛZ that maps $|0\rangle|0\rangle$, $|0\rangle|1\rangle$, $|1\rangle|0\rangle$, and $|1\rangle|1\rangle$ to $|0\rangle|0\rangle$, $|0\rangle|1\rangle$, $|1\rangle|0\rangle$, and $-|1\rangle|1\rangle$, respectively. The remaining problem is to obtain a procedure for implementing ΛZ (up to Pauli operations) using only the one-qubit projective measurement corresponding to the axis $(\cos\theta)X+(\sin\theta)Y$ for any $\theta\in[0,2\pi)$. Though it is difficult to implement ΛZ directly, I can show that there is a two-qubit unitary operation similar to ΛZ such that combining it with one-qubit unitary operations implements an arbitrary unitary operation and that it can be implemented by using only Y-measurements. Thus, the set consisting of the one-qubit projective measurement corresponding to the axis $(\cos\theta)X+(\sin\theta)Y$ for any $\theta\in[0,2\pi)$ is sufficient for universal quantum computation.

4. Conclusions and future work

I examined the problem of minimizing the resources required for universality in measurement-only quantum computation and described a small set of projective measurements sufficient for universal quantum computation. A key ingredient of my procedures is state transfer based on the Y-measurements. It would be interesting to consider approximate universality in measurement-only quantum computation [10] because a small approximately universal set of projective measurements is particularly important in practice. Moreover, it would be interesting to investigate the resources required for other important problems, such as graph state preparation [9].

References

[1] M. A. Nielsen and I. L. Chuang, "Quantum Computation and Quantum Information," Cambridge University Press, 2000.

[2] Y. Takahashi, "Quantum Arithmetic Circuits: a Survey," IEICE Trans. Fundamentals, Vol. E92-A, No. 5, pp. 1276–1283, 2009.

[3] D. Gottesman and I. L. Chuang, "Demonstrating the Viability of Universal Quantum Computation Using Teleportation and Single-qubit Operations," Nature, Vol. 402, pp. 390–393, 1999.

[4] M. A. Nielsen, "Quantum Computation by Measurement and Quantum Memory," Phys. Lett. A, Vol. 308, No. 2-3, pp. 96–100, 2003.

[5] D. W. Leung, "Quantum Computation by Measurements," International Journal of Quantum Information, Vol. 2, No. 1, pp. 33–43, 2004.

[6] S. Perdrix, "State Transfer Instead of Teleportation in Measurement-based Quantum Computation," International Journal of Quantum Information, Vol. 3, No. 1, pp. 219–223, 2005.

[7] A. M. Childs, D. W. Leung, and M. A. Nielsen, "Unified Derivations of Measurement-based Schemes for Quantum Computation," Phys. Rev. A, Vol. 71, No. 3, 032318, 2005.

[8] P. Jorrand and S. Perdrix, "Unifying Quantum Computation with Projective Measurements Only and One-way Quantum Computation," Proc. of SPIE Quantum Informatics 2004, Vol. 5833, pp. 44–51, 2005.

[9] Y. Takahashi, "Simple Sets of Measurements for Universal Quantum Computation and Graph State Preparation," International Journal of Quantum Information, Vol. 8, No. 6, pp. 1001–1012, 2010.

[10] S. Perdrix, "Towards Minimal Resources of Measurement-based Quantum Computation," New Journal of Physics, Vol. 9, No. 6, 206, 2007.

Yasuhiro Takahashi

Scientist, Computing Theory Research Group, Innovative Communication Laboratory, NTT Communication Science Laboratories.

He received the B.S. and M.S. degrees in mathematics from Tohoku University, Miyagi, and the Ph.D. degree in engineering from the University of Electro-Communications, Tokyo, in 1998, 2000, and 2008, respectively. He joined NTT Communication Science Laboratories in 2000 and has been engaged in research on the design and optimization of quantum circuits including measurement-based ones. His research interests include quantum computing, computational complexity theory, and cryptography. He is a member of the Information Processing Society of Japan and the Institute of Electronics, Information and Communication Engineers.

Speech Dereverberation Using Linear Prediction

Keisuke Kinoshita† *and Tomohiro Nakatani*

Abstract

This article describes a method of reducing reverberation in an observed signal to mitigate problems experienced in speech communication systems, such as hands-free mobile telephones, videoconferencing systems, hearing aids, and voice-controlled robots. It focuses on dealing with the effect of late reverberations, which are known to be a major cause of the degradation of automatic speech recognition (ASR) performance and loss of speech intelligibility. Experimental results show that this method can provide substantial improvements in ASR performance and audible quality under severely reverberant conditions.

1. Introduction

The last decade has seen the rapid development and pervasiveness of speech technologies, such as hands-free (mobile) telephones, videoconferencing, and hearing aids. In the near future, we can expect to see a dramatic spread of human-machine communication systems, for example, voice-operated electrical appliances and intelligent communication robots, which have already been partially launched and are attracting attention in the market. The main user benefit of hands-free telephones is that they enable the user to walk around freely without wearing a headset or microphone, so they provide a natural communication style. Users of hearing-aid applications obviously benefit from better hearing capability that helps them to interact more fluently with other people. The realization of communication robots will undoubtedly lead to numerous innovative services and technologies, and the benefits brought by these technologies will be literally beyond our imagination.

In all these examples, the position of the target speaker can be at a considerable distance from the microphone. As a result, the observed signal at the microphones can be degraded by reverberation caused by reflection from walls, floors, ceilings, and furniture. The reverberant speech signal recorded at the m-th microphone is generally modeled as:

$$x_m(n) = \sum_{k=0}^{L-1} h_m(k)s(n-k), \quad (1)$$

$$=[s*h_m](n), \quad (2)$$

where $s(n)$ denotes clean speech and $h_m(n)$ the room impulse response (RIR) between the source signal and the m-th microphone, which is assumed to be time invariant in this article. $[f*g](n)$ stands for the convolution of f and g. The acoustic system treated in Eq. (1) is shown in **Fig. 1**. A dereverberation method is generally applied to the received microphone signal $x_m(n)$ to estimate the desired signal $s(n)$. It should be noted that most of the existing acoustic signal processing techniques, e.g., automatic speech recognition (ASR), source separation techniques, and noise reduction techniques [1]–[6], completely fail or experience dramatically reduced performance when reverberation is present. In addition, even after a considerable number of investigations, dereverberation in real environments still remains one of the most challenging speech signal processing tasks to this day. Thus, the investigation of dereverberation algorithms is evidently important.

Reverberant speech is generally assumed to consist of three parts: a direct-path response, early reflections, and late reverberation. In this article, the early

† NTT Communication Science Laboratories
Soraku-gun, 619-0237 Japan

reflections are defined as the reflection components that arrive after the direct-path response within a time interval of about 30 ms, and the late reverberation as all the latter reflections. Since late reverberation is known to be a major cause of ASR performance degradation and speech intelligibility loss, this article focuses on dealing with the effect of late reverberation. The two most serious detrimental effects caused by late reverberation are summarized below.

(1) Effects on waveform and spectrogram

The effects of late reverberation on speech are clearly visible in the spectrogram and waveform representation. The spectrogram and waveform of an anechoic speech signal are depicted in **Fig. 2(a)**. The phonemes are well separated in time. Now, if the anechoic signal in Fig. 2(a) is reverberated, for instance, with the RIR measured in an office at a distance of 0.5 m from the source, the received signal tends to show the characteristics shown in **Fig. 2(b)**. In Fig. 2, we simulated a situation with RT_{60} of about 0.6 s, where RT_{60} is the time required for reflections of a direct sound to decay by 60 dB below the level of the direct sound. The smearing of the phonemes in time is clearly noticeable in both the spectrogram and the waveform. Owing to this smearing, the empty spaces between words and syllables are filled up, and subsequent phonemes overlap [7]–[9]. These distortions result in an audible difference between the anechoic speech and the reverberant speech and lead to degraded speech intelligibility and fidelity. These detrimental perceptual effects are primarily caused by late reverberation, and they generally increase with increasing distance between the source and microphone.

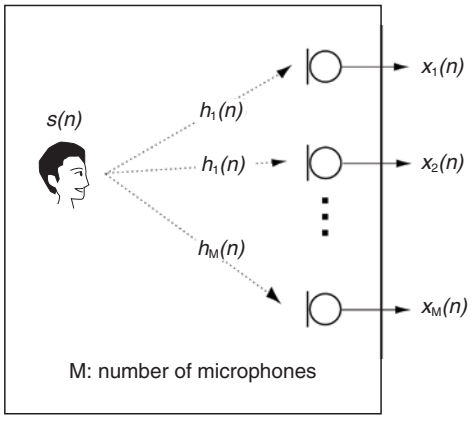

Fig. 1. Acoustic system treated here.

(2) Effect on ASR performance

The performance of ASR systems depends heavily on the quality of the input speech. While reasonable recognition performance is commonly achieved when the source-microphone distance is small, the performance tends to decrease drastically as the distance increases. To explain the reason, we show a block diagram of a typical speech recognition system in **Fig. 3**. In the system, first, acoustic features such as Mel frequency cepstral coefficients (MFCCs) are extracted from the speech signal using a short time frame (e.g., 30 to 50 ms) of the speech signal. These

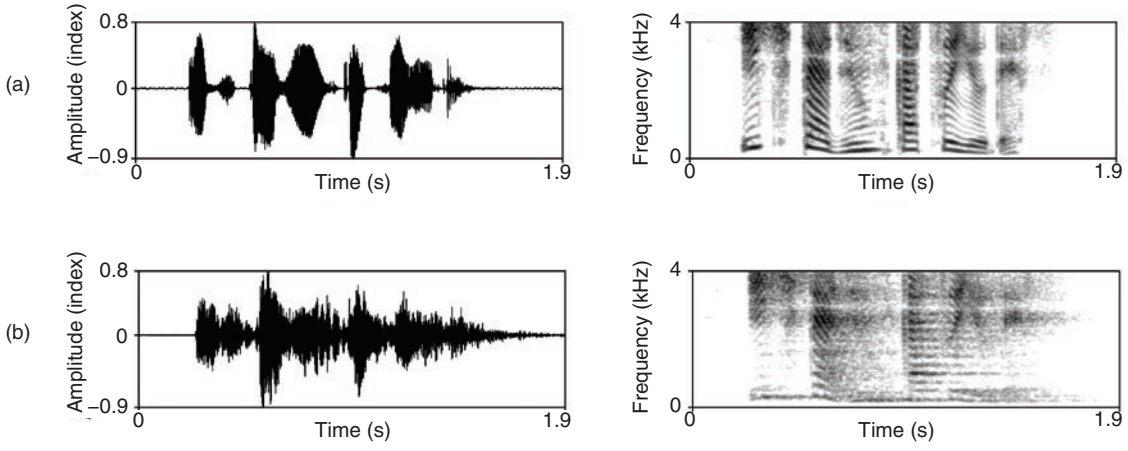

Fig. 2. Waveforms and spectrograms of (a) clean speech signal and (b) reverberant speech signal.

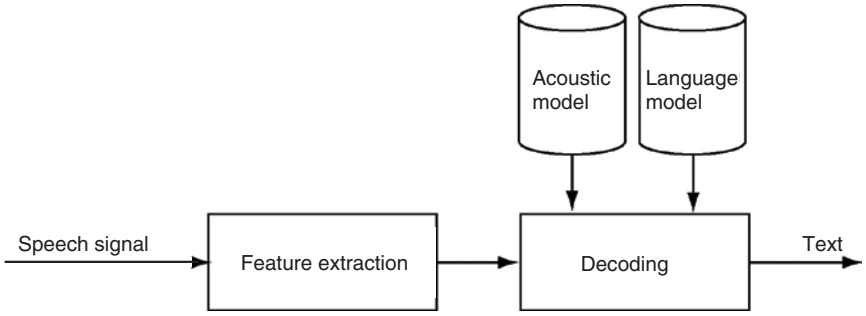

Fig. 3. Typical ASR system configuration.

acoustic features are meant to characterize the essential information present in the speech signal. Next, on the basis of these acoustic features, the most likely text is found by the decoder using two types of knowledge sources: an acoustic model and a language model. The acoustic model contains acoustic knowledge required to decode the features into phonemes, and the language model contains linguistic knowledge required to decode these phonemes into words or sentences. These models should be trained using a set of training data prior to the decoding step. In most cases, the acoustic model is trained on a set of acoustic features extracted from a clean (i.e., undistorted) speech signal. Thus, if the input signal to the ASR system is distorted, for example, by reverberation, the acoustic model mismatches the input signal, which leads to degraded recognition performance.

The influence of reverberation on the performance of a state-of-the-art speech recognition system [10], which has been developed at NTT Communication Science Laboratories, is shown in **Fig. 4**. The word error rate (WER) of continuous speech recognition is shown for various distances in an environment with a reverberation time of 0.6 s. The reverberant signals were generated by convolving anechoic speech signals taken from the Japanese newspaper article speech (JNAS) corpus [11] with a synthetic RIR. The solid line represents the WER for reverberant speech, while the star (★) shows that for clean speech for reference. Note that in this figure, the WER increases with increasing source-microphone distance. From this simple example, it is clear that the effects of reverberation on the ASR system are rather severe. Similar results are obtained if the reverberation time is varied, for example, from 0.1 s to 1.0 s with a fixed microphone-source distance of 1 m.

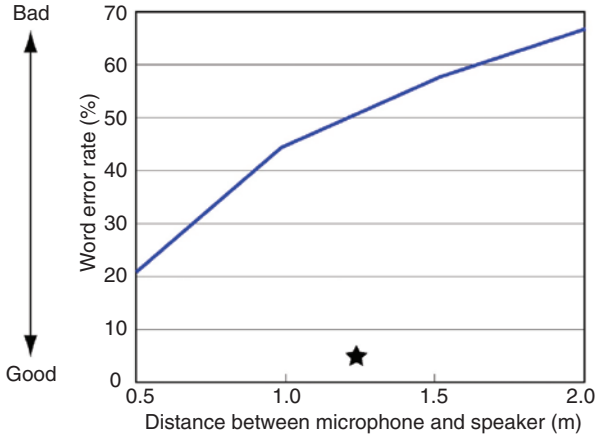

Fig. 4. Tendency of the WER in a reverberant environment. The solid line represents the WER of the reverberant speech, while the star represents that of clean speech.

2. Difficulty of speech dereverberation

The problem of speech dereverberation has been viewed as one of the most difficult tasks in the field of acoustic signal processing research. To explain the difficulty of speech dereverberation, we show the process of reverberant speech generation in **Fig. 5**. As you can see from the figure, first, the clean speech signal $s(n)$ is generated as a convolution of white noise $u(n)$ and the impulse response of the vocal tract filter $\alpha(n)$, i.e., $s(n)=[u*\alpha](n)$, and then the reverberant speech $x_m(n)$ is generated according to Eq. (2). That is, the observed signal $x_m(n)$ can be alternatively formulated as

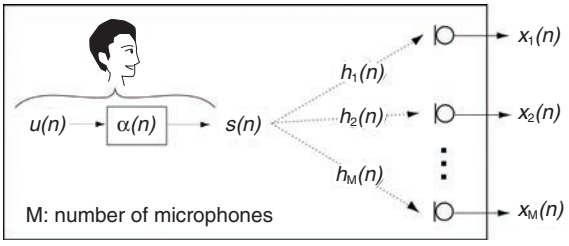

Fig. 5. Process of clean speech and reverberant speech generation.

$$x_m(n)=[u*\alpha*h_m](n). \quad (3)$$

To recover the clean speech $s(n)$ with the observation of only $x_m(n)$, it is necessary to distinguish two unknown impulse responses contained in the observed signal, i.e., $\alpha(n)$ and $h_m(n)$, and remove only the effect due to $h_m(n)$. Since it is not trivial to distinguish these two unknown impulse responses on the basis of only the observed signal, speech dereverberation problem has remained as unsolved problem for many years.

Some researchers have proposed a subspace method for estimating the RIRs by distinguishing these two unknown impulse responses [12]. This method can work effectively in the case of a well-conditioned problem, where the order of the RIR is small and its inverse filter can be calculated in a numerically stable manner. However, real reverberant environments are generally regarded as ill-conditioned problems, where the RIR order is more than several thousand milliseconds, and the calculation of its inverse filter often becomes numerically unstable. Therefore, the subspace method could not work effectively with real recordings. In this article, we propose a dereverberation algorithm that can appropriately distinguish the abovementioned two unknown impulse responses even in the case of an ill-conditioned problem. Thus, it is suitable for speech dereverberation.

3. Dereverberation based on multichannel linear prediction

It is known that linear prediction algorithms [13] are very powerful for estimating the inverse filter of the unknown system. One advantage of using linear prediction is that it is very robust in the case of ill-conditioned problems. However, the conventional linear prediction algorithm does not have mechanism for distinguishing two unknown impulse responses included in the observation process, so it cannot be used for the speech dereverberation as it is. To make the linear prediction algorithm suitable for speech signal dereverberation, in this section, we introduce a dereverberation algorithm based on the *generalized* linear prediction algorithm, namely multi-step linear prediction (MSLP) [14].

MSLP is designed to estimate and suppress only late reverberation, appropriately distinguishing it from the vocal tract filter $\alpha(n)$. Importantly, the length of the vocal tract filter $\alpha(n)$ is, in general, relatively short compared with that of the RIR $h_m(n)$, such as 30 to 100 ms, while the RIR length can be several hundred milliseconds or sometimes more than a second. By taking advantage of this inherent speech property, i.e., the difference in the lengths of two unknown impulse responses, we can correctly estimate the late reverberation which arrives after the direct path-response with a delay of more than the length of $\alpha(n)$.

First, let us modify Eq. (1) to clearly define the late reverberation component to be estimated with MSLP:

$$\begin{aligned} x_m(n) &= \sum_{k=0}^{D-1} h_m(k)s(n-k) + \sum_{k=D}^{L-1} h_m(k)s(n-k), \\ &= d_m(n)+r_m(n), \end{aligned} \quad (4)$$

where D is the step-size parameter used in MSLP, $d_m(n)$ denotes the mixture of the direct signal and early reflections, and $r_m(n)$ denotes the late reverberation. Now, if the room transfer function does not share common zeros, it is known that the above equation can be reformulated into the following autoregressive process using multichannel MSLP:

$$x_m(n) = \sum_{i=1}^{M}\sum_{k=0}^{K-1} w_{m,i}(k)x_i(n-D-k) + d_m(n), \quad (5)$$

where K is the length of the linear prediction filter, M is the number of microphones, and $w_{m,i}(n)$ are the prediction coefficients used to predict the observed signal at the m-th microphone at the present time using the past observed signals at the i-th microphone. As we can see from Eq. (5), the observed signal $x_m(n)$ can be expressed as the addition of the signal components that can be predicted from the past observed signal, and the direct signal plus the early reflections, $d_m(n)$, which cannot be predicted from the past observed signal. Note that, we can also see that, by comparing Eqs. (4) and (5), the first term in Eq. (5) can be regarded as the estimate of the late reverberation component. After estimating the prediction coefficients, we can suppress the late

reverberation as in the following inverse filtering form

$$\hat{s}_1(n) = x_1(n) - \sum_{i=1}^{M} \sum_{k=0}^{K-1} w_{1,i}(k) x_i(n-D-k) \quad (6)$$

For simplicity, with Eq. (6), we show only the case of suppressing the late reverberation contained in $x_1(n)$.

Needless to say, it is essential to estimate $w_{m,i}(n)$ as accurately as possible in order to efficiently suppress the late reverberation. In [14], the minimum mean square error criterion is presented for estimating $w_{m,i}(n)$ as

$$\mathrm{w}_1 = E\{x(n-D)x(n-D)^T\}^+ E\{x(n-D)x_1(n)^T\}, \quad (7)$$

where

$$\mathrm{x}(n) = [\mathrm{x}_1(n)^T, \mathrm{x}_2(n)^T, \ldots, \mathrm{x}_M(n)^T],$$
$$\mathrm{x}_m(n) = [x_m(n), x_m(n-1), \ldots, x_m(n-L+1)],$$
$$\mathrm{w}_m = [\mathrm{w}_{m,1}^T, \mathrm{w}_{m,2}^T, \ldots, \mathrm{w}_{m,M}^T]^T,$$
$$\mathrm{w}_{m,i}^T = [\mathrm{w}_{m,i}(0), \mathrm{w}_{m,i}(1), \ldots, \mathrm{w}_{m,i}(L-1)]^T.$$

With this estimation scheme, we can show that the linear prediction coefficients for achieving accurate dereverberation can be obtained if step-size parameter D is set as $\mathrm{D} > T_S$, where T_S is defined as

$$E\{s(n)s(n')\} = 0 \text{ if } |n-n'| > T_S . \quad (8)$$

Here, T_s corresponds to the maximum period of time during which the clean speech signal is assumed to maintain a non-negligible autocorrelation value. It should be noted that the clean speech signal is known to have a larger autocorrelation value only within a short-time region due to the characteristics of the vocal tract. In other words, while the short-term correlation of *reverberant* speech can be affected by both clean speech signal component and early reflection, its long-term correlation is mostly dominated by only the late reverberation effect. Since T_S corresponds roughly to the length of the vocal tract filter $\alpha(n)$ if we set D sufficiently larger than the length of $\alpha(n)$, MSLP can efficiently utilize the long-term correlation as in Eq. (7) and estimate the late reverberation precisely, distinguishing it from the vocal tract filter $\alpha(n)$. With our experiment, we found that the method could estimate an accurate late reverberation component when we used D of 30 ms.

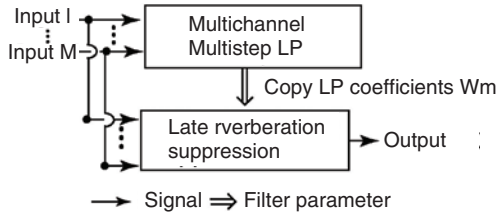

Fig. 6. Schematic diagram of our method.

The processing diagram of our dereverberation method based on multichannel MSLP is shown in **Fig. 6**. First, using multichannel MSLP, we estimate the prediction coefficients for estimating late reverberations at the i-th microphone. Then, on the basis of the estimated coefficients, we perform inverse filtering as in Eq. (6) to achieve the dereverberation. A more robust way of achieving this inverse filtering is presented in [14], and its efficiency has been demonstrated.

4. Dereverberation experiments

We carried out dereverberation experiments in severely reverberant environments and evaluated the performance of our method in terms of spectrograms and ASR performance.

Spectrograms of clean speech, reverberant speech at a distance of 1.5 m, and speech dereverberated by our method using four microphones are shown in **Fig. 7**. The effect of the method can be clearly seen. The harmonic structure of the speech signal is well restored, and the separation of the phonemes in time is well reconstructed. The improvement in audible quality can be confirmed in [15]. The WER as a function of the distance between the microphone and speaker is shown in **Fig. 8**. The dashed line shows the WER of the reverberant speech, and the solid line shows that of the signal processed by our method. The recognition result for clean speech is also plotted by the star (★) as a reference value for the lowest possible WER, i.e., 4.4%, that can be achieved with this ASR system for this recognition task. As seen from the figure, if the reverberant speech is not subjected to any preprocessing, the WER increases greatly with distance. Our method achieved a substantial reduction in the WER for all the tested reverberant conditions.

5. Concluding remarks

A speech signal captured by a distant microphone is smeared by reverberation, which severely degrades the ASR performance and the audible quality of speech signal. In this article, we introduced a novel

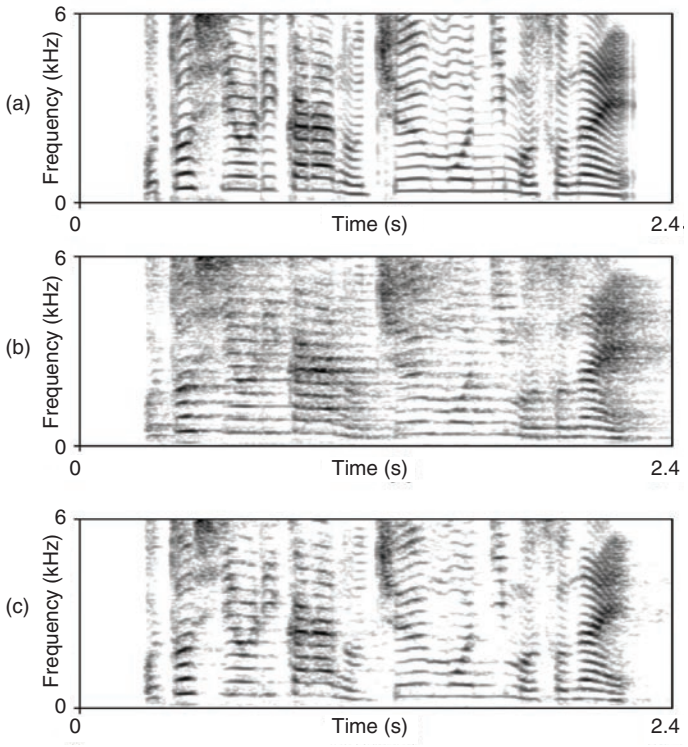

Fig. 7. Spectrograms of (a) clean speech, (b) reverberant speech, and (c) speech dereverberated by our method using four microphones.

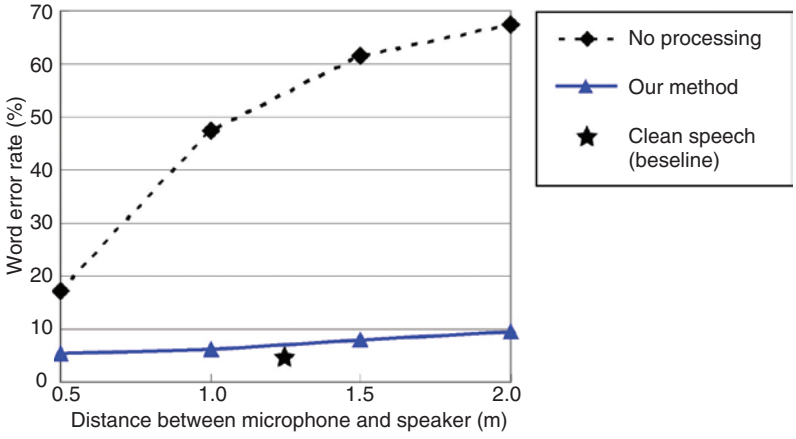

Fig. 8. WER as a function of distance between microphone and speaker.

dereverberation method based on the multichannel linear prediction and showed its efficiency. It can be used, for example, as an efficient preprocessor for ASR system and as a useful speech enhancement tool for audio postproduction engineers [15].

References

[1] J. Benesty, S. Makino, and J. Chen, "Speech Enhancement," Springer-Verlag, New York, NY, USA, 2005.
[2] T. F. Quatieri, "Discrete-time Speech Processing: Principles and Practice," Prentice Hall, Upper Saddle River, NJ, USA, 1997.
[3] M. Brandstein and D. Ward, "Microphone Array," Springer-Verlag, New York, NY, USA, 2001.
[4] H. L. V. Trees, "Optimum Array Processing," Wiley-Interscience, New York, NY, USA, 2002.
[5] S. Haykin, "Adaptive Filter Theory, 3rd ed.," Upper Saddle River, NJ: Prentice-Hall, 1996.
[6] S. Haykin ed., "Unsupervised Adaptive Filtering: Blind Source Separation," Wiley-Interscience, New York, NY, USA, 2000.
[7] V. O. Knudsen, "The Hearing of Speech in Auditoriums," J. Acoust. Soc. Am., Vol. 1, No. 1, pp. 56–82, 1929.
[8] R. H. Bolt and A. D. MacDonald, "Theory of Speech Masking by Reverberation," J. Acoust. Soc. Am., Vol. 21, No. 6, pp. 577–580, 1949.
[9] A. K. Nábélek, R. Letowski, and F. M. Tucker, "Reverberant Overlap- and Self-masking in Consonant Identification," J. Acoust. Soc. Am., Vol. 86, No. 4, pp. 1259–1265, 1989.
[10] T. Hori, C. Hori, Y. Minami, and A. Nakamura, "Efficient WFST-based One-pass Decoding with On-the-fly Hypothesis Rescoring in Extremely Large Vocabulary Continuous Speech Recognition," IEEE Trans. Speech, Audio and Language Processing, Vol. 15, No. 4, pp. 1352–1365, 2007.
[11] "JNAS: Japanese Newspaper Article Sentences," (in Japanese). http://www.mibel.cs.tsukuba.ac.jp/_090624/jnas/
[12] S. Gannot and M. Moonen, "Subspace Methods for Multi Microphone Speech Dereverberation," EURASIP Journal of Applied Signal Process., Vol. 2003, No. 11, pp. 1074–1090, 2003.
[13] T. Kailath, A. H. Sayed, and B. Hassibi, "Linear Estimation," Upper Saddle River, NJ: Prentice Hall, 2000.
[14] K. Kinoshita, M. Delcroix, T. Nakatani, and M. Miyoshi, "Suppression of Late Reverberation Effect on Speech Signal Using Long-term Multiple-step Linear Prediction," IEEE Trans. Audio, Speech, and Language Processing, Vol. 17, No. 4, pp. 534–545, 2009.
[15] Sound demonstration of the speech dereverberation software developed on the basis of the principle presented in this article. http://www.tacsystem.com/en/products/softwares/000563.php

Keisuke Kinoshita
Researcher, NTT Communication Science Laboratories.
He received the M.Eng. and Ph.D. degrees from Sophia University, Tokyo, in 2003 and 2010, respectively. Since joining NTT Communication Science Laboratories in 2003, he has been engaged in research on speech and audio signal processing. His research interests include speech enhancement, robust automatic speech recognition, and music signal processing. He received the 2006 IEICE Paper Awards and the 2009 ASJ Technical Development Awards. He is a member of IEEE, Acoustical Society of Japan (ASJ), and the Institute of Electronics, Information and Communication Engineers (IEICE).

Tomohiro Nakatani
Senior Research Scientist, Supervisor, NTT Communication Science Laboratories.
He received the M.Eng. and Ph.D. degrees from Kyoto University in 1991 and 2002, respectively. Since joining NTT as a researcher in 1991, he has been investigating speech enhancement technologies for developing intelligent human–machine interfaces. He received the 2006 IEICE Paper Award and the 2009 ASJ Technical Development Award. He has been a member of the IEEE Signal Processing Audio and Acoustics Technical Committee since 2009. He is a senior member of IEEE and a member of IEICE and ASJ.

Virtual Private Network Authentication System Featuring High Extensibility and Availability: AAA

Kenichi Matsui†, *Kenji Ota, Hiroyuki Kurita, Hitoshi Nagao, Kenichi Mase, and Shinya Matsumoto*

Abstract

NTT Network Service Systems Laboratories has developed an authentication system, called AAA, that authenticates users when they try to access a virtual private network (VPN). It features both high extensibility, which is the ability to flexibly combine multiple authentication methods depending on how a given user uses a VPN service, and high availability, which is the ability to avoid service disruption even in the event of a serious disaster.

1. Introduction

As the computerization of office operations advances, it has become common to interconnect local area networks in multiple office sites to carry out office operations in an integrated manner. This interconnection is increasingly being done using virtual private network (VPN) services, which are cheaper than leased-line services. In Japan, the use of VPNs now surpasses that of leased lines, especially in the case of enterprise users: about half of all enterprise users now opt for VPNs [1].

Unlike leased lines, VPNs are configured on a public network, which can be accessed by the general public. Therefore, an authentication system is needed to ascertain that someone trying to access a VPN has the authority to do so.

A VPN authentication system must provide three basic functions: an authentication function to identify the user correctly, an authorization function to check whether the user has the authority to use the requested service according to the contract with the user, and an accounting function to record the user's usage. These three functions are collectively known as AAA. A VPN authentication system equipped with these functions can authenticate users, determine whether or not the user should be permitted to access a given service, and manage usage records for all users.

Although VPN authentication systems normally use only a user ID (identification) and password for authentication and authorization, rising concerns about security are leading to demands for the use of multiple authentication factors, such as identification of the user's access line, in addition to user ID and password [2]. VPN authentication systems are required to be able to provide different combinations of authentication and authorization flexibly depending on the needs of each service.

As VPN services become widely utilized, an increasing number of enterprises are applying VPNs to systems that require high availability, such as their core business systems, but a failure in such systems could cause considerable damage. Therefore, VPN authentication systems need to provide high availability to avoid service disruption even in the event of

† NTT Network Service Systems Laboratories
Musashino-shi, 180-8585 Japan

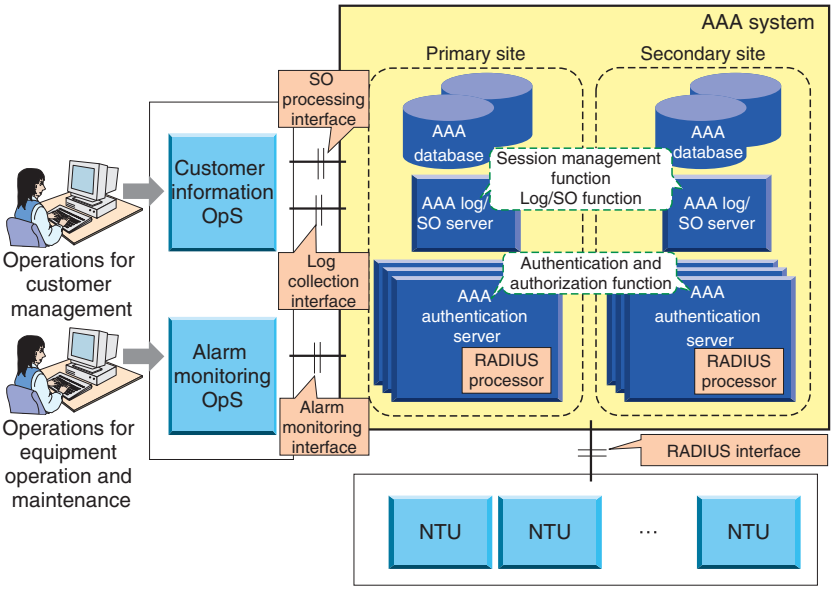

Fig. 1. Overall configuration of AAA.

a serious disaster.

To meet these requirements, we have developed a VPN authentication system, called AAA, that has high extensibility and availability in processing authentication and authorization. This article describes the configuration, functions, and features of this system, which has already been implemented.

2. System configurations and functions

2.1 Configuration

The overall configuration of our system is shown in **Fig. 1**. The AAA consists of three parts. The AAA authentication server performs authentication and authorization. The AAA log/SO server collects and formats logs, processes service orders (SOs), which are users' service provisioning requests, in collaboration with the operations system (OpS), and manages session information. The AAA database stores information about authentication derived from service orders, information about equipment, and information about established sessions.

In preparation for serious disasters, the AAA is duplicated at two sites. The number of AAA authentication servers can vary depending on the number of connected network termination units (NTUs), which control user terminals.

2.2 Authentication and authorization functions

The AAA exchanges authentication information with NTUs using RADIUS (Remote Authentication Dial-In User Service), which is a user authentication security protocol. The basic operation of the system up to the establishment of a VPN connection is as follows (**Fig. 2**):

(1) The router or home gateway in the user network sends the user ID and password to the NTU to request a VPN connection.

(2) The NTU requests the AAA to authenticate the user using the network information (e.g., line identification) that it possesses, in addition to the user ID and password.

(3) The AAA determines whether the connection should be permitted by referring to the authentication and authorization request from the network terminal unit and the user's authorization conditions stored in the database. It sends its decision back to the NTU.

(4) The NTU either starts or rejects the requested VPN connection depending upon the reply from the AAA. If a connection is to be started, the NTU asks the AAA to start recording the session for accounting. The AAA records the session information, which shows the state of the user's connection (access line identification, connection start time, IP address given, etc. (IP: Internet protocol)).

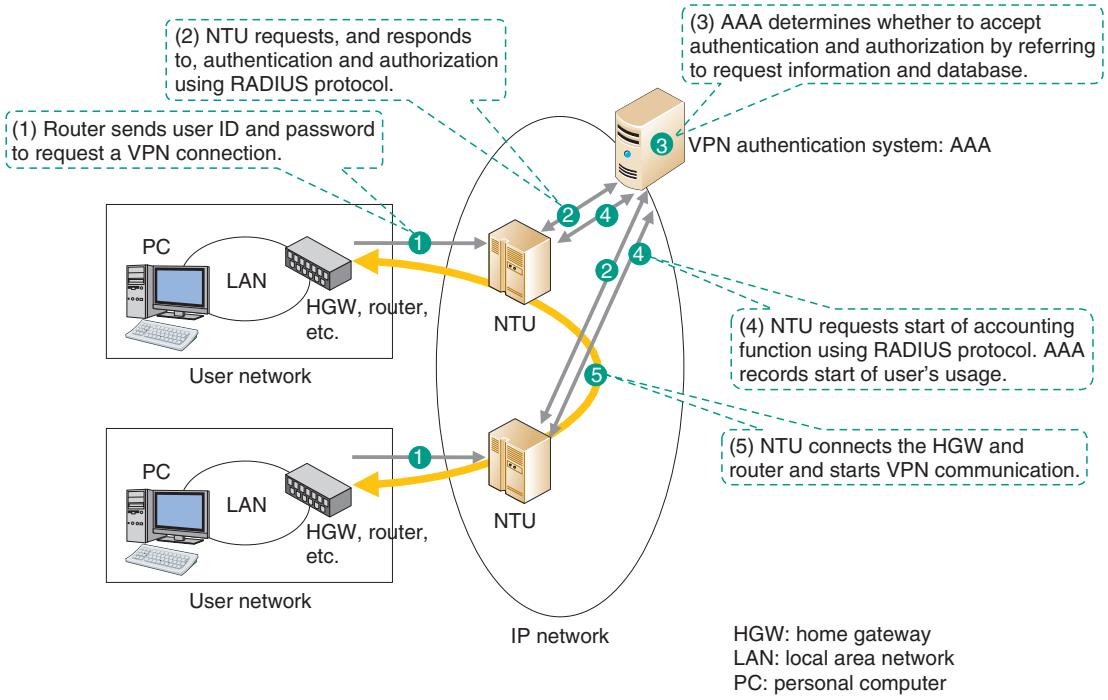

Fig. 2. Basic authentication operation up to VPN connection establishment.

(5) The NTU connects the user terminal, and VPN communication is started.

In this way, the AAA authenticates and authorizes VPN users in a highly secure manner on the basis of the user ID, password, and line identification (in this example).

2.3 VPN session management function

The AAA holds the session information about the user who has been connected to the VPN after authentication has been completed. This session information is used to prevent double logins from the same user and is also referred to when maintenance staff check the connection state to deal with a complaint from the user.

As the user's connection state changes (connection establishment or release), the session information held by the AAA is updated on the basis of information contained in RADIUS messages sent by the NTU. If the RADIUS messages fail to reach the AAA owing to packet loss or a fault in the NTU, the session information held by the AAA may become different from the user's actual connection state. To resolve such a discrepancy, the AAA collects the user's connection information from the NTU and automatically corrects the session information concerned. Specifically, this function operates as follows (**Fig. 3**):

(1) The AAA log/SO server obtains the session information list from the AAA database.
(2) It obtains the session information list from the NTU.
(3) It compares the two lists: if they do not match, it replaces the session information in the AAA database by that held by the NTU.

This session information correction can be executed without suspending the operation of the AAA and enhances the reliability of the session information. Session information can also be sent to devices other than the AAA for use in authentication by upper-layer applications, such as ASP (application service provider) services and SaaS (software as a service).

2.4 SO function

The SO function updates the SO information needed for VPN authentication in collaboration with the OpS. It registers, updates, deletes, or refers to SO information in the AAA database in response to an SO request sent by the OpS. In addition, it asks the NTU to release the user's session.

The SO function and the OpS exchange messages written in XML (extensible markup language) using

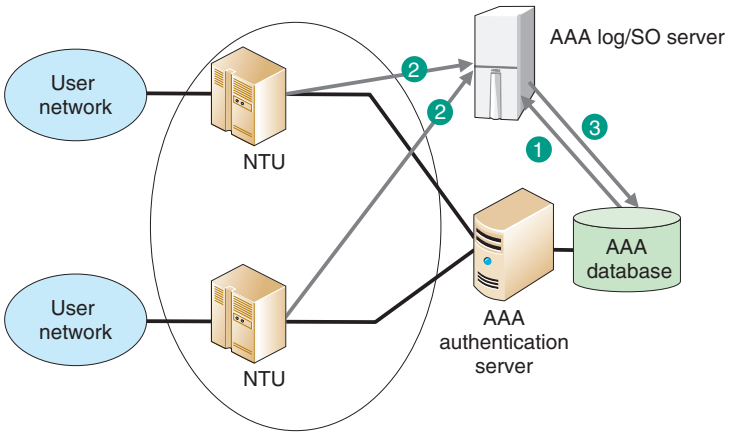

Fig. 3. Operation of session information correction.

the message exchange protocol SOAP (simple object access protocol) to ensure versatility and extensibility in authentication.

3. Features

3.1 Provision of usage history reports

The AAA can provide the history of each user's authentication and authorization in the form of a report.

The VPN authentication server normally outputs the information included in RADIUS messages sent from NTUs, to the authentication and authorization log. However, in a VPN service, which can be accessed from lines of various types, the NTUs used may also vary. Attributes included in RADIUS messages can vary depending on the type of NTU. Therefore, it is not straightforward to generate a usage history report from authentication and authorization logs.

To solve this problem, items that are output in usage history reports (events, such as the start and end of usage, date and time when each event occurred, user ID, line number, etc.) are defined for each type of NTU.

3.2 Extensibility of authentication and authorization function

The number of items that the authentication and authorization function must check is growing. To be able to cope with such an increase flexibly through the simple addition of necessary functions, the AAA has extended interfaces (**Fig. 4**).

The extended processing part obtains or changes information needed in the processing of authentication and authorization, such as user ID, password, and network information, through an extended interface. When a new authentication and authorization module is added, the module obtains the necessary information and returns processing results to the basic processing part through the extended interface so that the processing results will be reflected in the authentication and authorization. Since extended functions can be added without modification of the AAA's basic processing part, new authentication and authorization capabilities can be easily added to meet new user needs.

An extended interface is available for each of the three stages of processing: processing concerning all users, processing concerning only legitimate users, and processing concerning authorization. This arrangement makes it possible to select an extended interface appropriate for a specific processing operation or to select an appropriate method of adding functions in order to achieve high-speed processing. For example, processes executed for only legitimate users, such as authentication and authorization processes, for which the occurrence number is proportional to the number of user sessions, can be applied after the authentication of individual users. This will limit the number of users handled by these processes and thus eliminate wasteful processing.

3.3 Compatibility of availability and high-speed processing

In preparation for major disasters, the AAA has a redundancy configuration in which a system is installed at each of two sites: the primary site and the

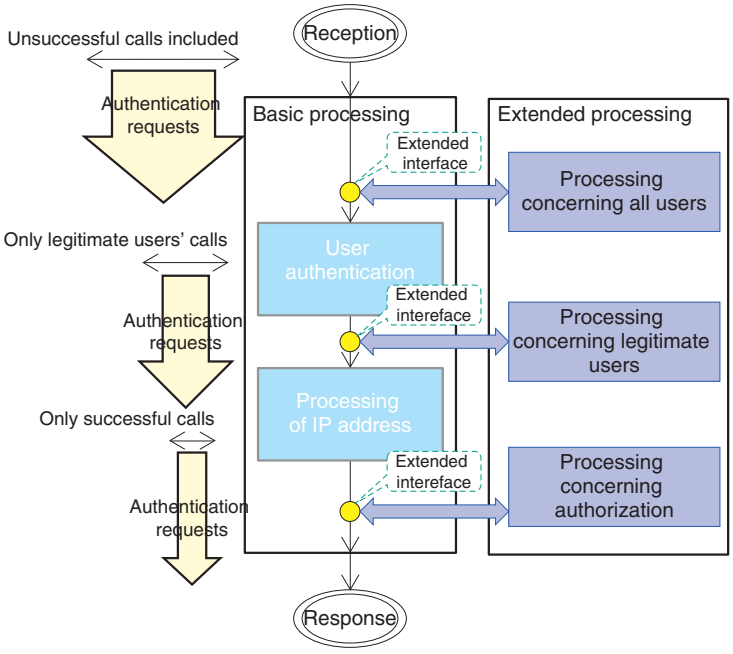

Fig. 4. Extensibility of the authentication/authorization process.

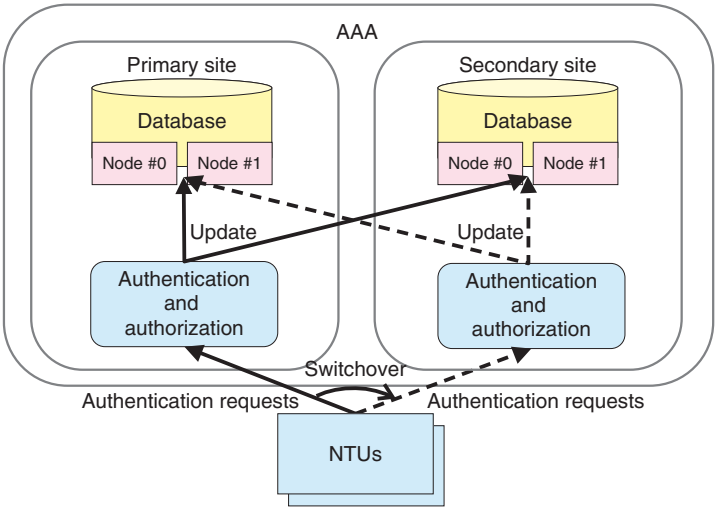

Fig. 5. Redundancy configuration of the AAA system.

secondary site (**Fig. 5**). Both systems are kept active. If the system at the primary site is disrupted, all NTUs switch over to the system at the secondary site, which continues to provide authentication and authorization.

To support the switchover to the secondary-site system, the databases at the two sites must be synchronized in real time to ensure consistency in the checking of double logins and other processing. To meet this requirement, database updating is executed at the two sites simultaneously so that the contents of the two databases are always synchronized. To enhance the authentication response performance, access to the databases is minimized. For example,

the system that has received a request for authentication refers only to its own database, and it sends an authentication reply to the requesting NTU only after it has successfully updated its database. The other database will be updated after the authentication reply has been sent. This arrangement makes it possible to keep duplicate data for authentication and authorization at two sites while ensuring high-speed authentication. For even higher availability, each site has a cluster of two data servers.

4. Conclusion

The AAA authenticates users when they try to access a VPN. It features both high extensibility and high availability. It is currently used in the FLET'S VPN Wide Service (offered by NTT EAST since August 2010 and by NTT WEST since November 2009). Building upon the core authentication technology developed through these research and development activities, we will study technologies that enable users to access a variety of network services on VPNs, such as ASP and cloud services, safely, securely, and conveniently.

References

[1] Nikkei BP, "Fact-finding Survey of Networks 2010," NIKKEI NETWORK, No. 123, pp. 046–047, July 2010 (in Japanese).
[2] B. Nagel, "Password Seeks Partner for Long-term, Secure Relationship," CIO, Vol. 11, No. 2, pp. 28–31, 2010.

Kenichi Matsui
Senior Research Engineer, Third Promotion Project, NTT Network Service Systems Laboratories.
He received the B.E. degree in information engineering and the M.S. degree in information sciences from Tohoku University, Miyagi, in 1995 and 1997, respectively. He joined NTT in 1997 and studied IP networking technology including IP multicast management, quality-of-service management, and traffic engineering. During 2005–2008, he was engaged in commercial development of IPTV and video-on-demand services. He is currently focusing on R&D of the Next Generation Network. He is a member of the Institute of Electronics, Information and Communication Engineers (IEICE), the Information Processing Society of Japan (IPSJ), and IEEE.

Kenji Ota
Research Engineer, Third Promotion Project, NTT Network Service Systems Laboratories.
He received the B.S. and M.S. degrees in mathematics from Keio University, Kanagawa, in 1989 and 1991, respectively. In 1991, he joined NTT Software Laboratories, where he engaged in R&D related to requirement engineering. He has been engaged in R&D concerning software engineering, IPv6 network operations, and secure network access. During 2001–2004, he was engaged in developing commercial services for the Global IP-VPN. His work is currently focused on R&D of the Next Generation Network. He is a member of IPSJ.

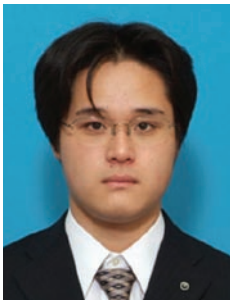

Hiroyuki Kurita
Engineer, Third Promotion Project, NTT Network Service Systems Laboratories.
He received the B.E. and M.E. degrees in information and communication engineering from the University of Tokyo in 2005 and 2007, respectively. He joined NTT Information Sharing Platform Laboratories in 2007 and studied network security including authentication and network attachment control. His work is currently focused on R&D of the Next Generation Network. He is a member of IEICE.

Hitoshi Nagao
Senior Research Engineer, Third Promotion Project, NTT Network Service Systems Laboratories.
He received the B.E. degree in information engineering from Tokushima University in 1993. He joined NTT in 1993. He is currently focusing on R&D of the Next Generation Network.

Kenichi Mase
Research Engineer, Third Promotion Project, NTT Network Service Systems Laboratories.
He received the B.E. degree in electrical engineering from Toyo University, Tokyo, in 1991. He joined NTT in 1991. He is currently focusing on R&D of the Next Generation Network.

Shinya Matsumoto
Research Engineer, Third Promotion Project, NTT Network Service Systems Laboratories.
He received the B.E. and M.E. degrees in electronics and electrical engineering from Doshisha University, Kyoto, in 1987 and 1989, respectively. He joined NTT Communication Switching Laboratories in 1989 and studied intelligent networks. His work is currently focused on R&D of the Next Generation Network.

NTT Com Asia

Total ICT Solutions Strengthen Hong Kong as the ICT Hub in Asia

Abstract

As the keystone of Mainland China, Hong Kong is powered by NTT Com Asia's comprehensive ICT (information and communications technology) solutions, which are strengthening its position as the regional ICT hub. It also supports the staggering growth of business activities in the region. This article introduces the office in Hong Kong and various ICT solutions offered.

1. Introduction

NTT Com Asia Limited (NTT Com Asia) [1] was established in Hong Kong in 1999. As the key arm of NTT Communications' Asia operations, it has devoted its best efforts to becoming the premiere ICT Solution Partner for enterprises in Greater China. In collaboration with its affiliate HKNet Company Limited (HKNet) [2], NTT Com Asia offers the best connectivity, datacentre, enterprise hosting, cloud, and managed services in the region. It has positioned itself as the communication gateway for global enterprises to develop and manage their operations in Hong Kong and mainland China. NTT Com Asia and HKNet currently employ around 300 industry professionals, working in three offices in Hong Kong. Earlier in May, the company expanded its operations and opened a new branch in Macao to meet the growing demands in that city.

2. Total ICT solutions

2.1 Connectivity services

Utilising NTT Communications' Tier I IP backbone and the Arcstar™ private network, NTT Com Asia and HKNet offer a full array of global and local connectivity services in Hong Kong from MPLS (multiprotocol label switching), IPVPN (Internet protocol virtual private network), leased line, IPv4/IPv6 (IP versions 4 & 6) transit, and a content delivery network to teleconferencing services. Thanks to its prime location in Asia, Hong Kong has developed as a regional ICT and financial hub with tremendous demand for top-quality network services.

2.2 Datacentre and managed services

NTT Communications Hong Kong Data Centre [3] (**Fig. 1**) and HKNet Kwai Chung Data Centre [4], which were designed to world-class standards, offer the best-in-class datacentre service in the region. Both facilities are carrier neutral, providing highly diverse options, good coverage, and high-availability failover solutions.

Officially launched in 2009, NTT Communications Hong Kong Data Centre is a dedicated datacentre located in a highly secure and robust environment in Tai Po, Hong Kong. This state-of-the-art seven storey datacentre provides a world-class datacentre service with a total gross area of 212,100 sq. ft. (19,705 m^2) and optimal power and cooling systems. It was designed with a Tier III+ fully redundant infrastructure. Every aspect of the facility is equipped with at least N+1 redundancy, and a multiple-source and multiple-path design was used to ensure business continuity.

This facility is accredited with ISO 27001 and 9001 for its Information Security Management System and Quality Management. In addition to these ISO

Fig. 1. NTT Communications Hong Kong Data Centre.

certifications of its high standard of operation performance, NTT Com Asia has recently scooped the accolade of Silver Award for Best Green ICT [5] bestowed on the NTT Communications Hong Kong Data Centre at The Hong Kong ICT Awards 2011 for its green management approach and achievements. Given its success in improving energy efficiency by 10% in the past two years, NTT Com Asia set forth another ambitious target of a further 10% efficiency enhancement within this year.

Last year, NTT Communications announced its plan to develop a green efficient, premium Tier IV-ready datacentre [6] to meet the demands of the market. 30,000 m^2 of land in Tseung Kwan O, Hong Kong, was acquired for the purpose-built structure. Upon completion, the new datacentre will have a total gross floor area of 70,000 m^2, composed of two five-storey datacentre buildings and one six-storey office building. Scheduled to begin operations in 2013, it is expected to be the first Tier IV-ready datacentre in the city and the largest one developed by a datacentre service provider in the city, complementing Hong Kong's position as an ICT hub in Asia.

The company's expansion plans have accelerated to accommodate exceptional levels of demand. Clients include multinationals from the financial services, telecommunications, logistics, and technology sectors as well as information technology (IT) and web companies originating from more than fifteen countries, including mainland China.

NTT Com Asia also provides an array of Managed Services [7] and worldwide technical support worldwide 24 hours a day, 7 days a week.

2.3 Enterprise hosting

For over ten years, NTT Com Asia has striven to optimise solutions that help enterprises to maximise their IT resource usage and enhance their business operations. NTT Com Asia's Enterprise Hosting Services are highly flexible and designed to support rapid deployment and implementation in order to facilitate enterprises' IT initiatives on any scale from local ad hoc projects to extensive global initiatives.

It offers a comprehensive portfolio of enterprise-grade hosting services from managed infrastructure outsourcing to subscription-based cloud solutions. These solutions support the extension of IT capabilities such as storage and servers in real time over the network on an as-needed basis, which helps enterprises to operate efficiently and flexibly while at the same time meeting the demand for increased mobility.

NTT Com Asia's Cloud Hosting solutions utilise VMware's virtualisation technology and NTT Communications' top-notch datacentre and Tier 1 Global IP Network. The comprehensive portfolio of cloud services, including Global Virtualization Service, Virtual Infrastructure, Virtual Desktop, and Virtual Server Hosting, helps enterprises to build their cloud platform and achieves the highest level of agility and efficiency for their businesses.

3. R&D incubation centre

NTT Com Asia takes pride in developing a research and development (R&D) incubation centre in Asia to nurture ICT technologies and innovation in Asia. By creating innovative ideas and driving R&D development, it hopes to bring about a breakthrough in advanced technologies in the ICT industry and lay the foundations for the future.

Last year, it organised the first ICT for the Future R&D Forum in Hong Kong. This featured cutting-edge technologies from NTT's R&D Centres that have enabled industry leaders to remain resilient while still being at the forefront of the latest technological trends (**Figs. 2–5**). The forum showcased approximately 20 exhibits from NTT's R&D Centres covering a wide spectrum of areas from the pursuit of Technologies for Human Life and Society, Technologies for Business; Energy and Environment Technologies; and Science, Engineering, and Network Technologies.

There were also demonstrations and thought-provoking keynote speeches delivered by NTT's Noritaka Uji, Senior Executive Vice President; Dr. Katsuhiko Kawazoe, Vice President and Chief Producer; and Dr. Kenji Yokoyama, General Manager from the

Fig. 2. Noritaka Uji opened the ICT for the Future R&D Forum with a keynote address.

Fig. 3. NTT Com Asia unveiled cutting-edge technologies.

R&D Planning Department as well as guest speaker Professor Matthew Ming-Fai Yuen, Acting Vice-President for Research and Development of The Hong Kong University of Science and Technology.

The event provided a platform for the exchange of views and successfully attracted hundreds of leaders from top corporations and the research community. Through the incubation of technology seeds, we look forward to further strengthening the strategic position of Hong Kong as the region's ICT hub.

4. Looking forward

NTT Com Asia will continue to provide high-quality innovative ICT solutions to the strategic market in Hong Kong, Macao, and Greater China for NTT Communications. With the accelerating demand for total ICT solutions for enterprises in Asia, we are bullish about its outlook and will strive to further strengthen Hong Kong's position as the region's ICT hub.

Fig. 4. 4K Digital Cinema, the world's first digital cinema distribution and management system, drew wide attention.

Fig. 5. Interactive Digital Signage, which comprises SpotAd and NTT Docomo's Recommender System and presents customised ads according to realtime movement and customer preferences and profiles, was also popular.

References

[1] NTT Com Asia. http://www.ntt.com.hk
[2] HKNET. http://www.hknet.com
[3] NTT Communications Hong Kong Data Centre. http://www.hk.ntt.com/en/products/data-centre/hong-kong-data-centre.html
[4] http://www.hknet.com/en/ict-solution/hong-kong-data-centre/kwai-chung-data-centre/server-colocation.html
[5] http://www.hk.ntt.com/en/about-us/newsevents/press-releases/press-releases/article/ntt-com-asia-achieves-10-improvement-in-energy-efficiency-for-hong-kong-data-centre.html
[6] http://www.hk.ntt.com/en/about-us/newsevents/press-releases/press-releases/article/ntt-communications-closes-land-acquisition-the-first-service-provider-to-build-a-tier-iv-ready-dat.html
[7] http://www.hk.ntt.com/en/products/managed-services/managed-services.html

NTT COM ASIA — short column

Dim sum is gaining in popularity in Japan. It is a range of delightful Chinese snacks that are mostly served hot in bamboo baskets accompanied by Chinese tea. I am sure that most of you have tried it and gained at least an indirect taste of this cultural aspect of Hong Kong. People say that you have not really been to Hong Kong if you didn't try dim sum during your trip. Here, these delightful, mouth-watering snacks are consumed at breakfast and lunch. Some of my favourites are steamed shrimp dumplings, pork dumplings, barbecued pork buns, and beef balls. Seeing these mini arts pieces, which are handmade in bite sizes, you will learn a bit of the local culture in Hong Kong.

When you go into a Chinese restaurant at lunch time or at the weekend, you may find the noise and crowds intimidating, especially if you are a first timer. Dim sum restaurants in Hong Kong are busy, loud, and fast-paced. That is what makes them great, but the clamour and clatter can also be off-putting. I like this kind of group experience where a selection of dishes is ordered and shared around the table. Many of the tables in the restaurants, which are mostly round, can seat from four to eight or even twelve people. Sitting alone is rare.

Dim sum is served in bamboo baskets.

Steamed beef dumplings: one of my favourite dim sum

Soon after your order has been placed, the food arrives at your table fairly fast. Sometimes the bamboo baskets are stacked up high and even block your view of your companions. This actually makes the great experience of dining in a dim sum restaurant. Joining the gang and being part of the bustling environment is really fun.

The experience is an accurate reflection of Hong Kong culture. People here like sharing, straightforwardness, and speed. Efficiency is always the top priority. In the office, people always try to get things done in the quickest possible way, which is sometimes a contrast to the courtesy and sedate procedures of Japanese culture. Decision-making processes are amazingly quick and I enjoy working in the heart of Asia.

Hong Kong is a fast moving city, just like Tokyo in Japan or New York in the USA. People walk extremely fast, especially during office hours. The city also has a pleasant side. The world-famous dazzling Victoria Harbour and relaxing country parks are some of the areas that I am fond of for outings.

View of Victoria Harbour from The Peak.

Tsing Ma Bridge.

Hong Kong is truly a gourmet's delight. I am sure that NTT Com Asia staff members will be delighted to recommend some of their favourite dishes during your next visit to Hong Kong.

Lucy Leung, NTT Com Asia Ltd.

External Awards

Commendation for Science and Technology by the Minister of Education, Culture, Sports, Science and Technology, The Young Scientist's Prize

Winner: Yoshitaka Taniyasu, NTT Basic Research Laboratories
Date: Apr. 23, 2011
Organization: The Ministry of Education, Culture, Sports, Science & Technology in Japan

For "Research on Crystal Growth of Aluminum Nitride and Its Application to Deep Ultraviolet Light-emitting Device".

Dr. Taniyasu has grown n-type and p-type aluminum nitride (AlN) layers for the first time to apply them to semiconductor devices. Using these layers, he has successfully demonstrated an AlN p-n junction light-emitting diode with a wavelength of 210 nm, the shortest ever reported for semiconductor solid-state light sources.

The Institute of Physics (IOP) Fellow

Winner: Hiroshi Yamaguchi, NTT Basic Research Laboratories
Date: May 18, 2011
Organization: Institute of Physics

For personal contribution to the advancement of physics as a discipline and a profession.

The Council of the Institute is concerned to ensure that the Fellowship of the Institute includes all those who have made an important contribution to physics, to the profession of physicist, or as physicists in their chosen career.

Best Paper Award

Winners: Ryogo Kubo[*1], Jun-ichi Kani[*2], Yukihiro Fujimoto[*2], Naoto Yoshimoto[*2], and Kiyomi Kumozaki[*3]

*1 Keio University
*2 NTT Access Network Service Systems Laboratories
*3 Mitsubishi Electric Corporation

Date: May 19, 2011
Organization: Institute of Physics

For "Adaptive Power Saving Mechanism for 10 Gigabit Class PON Systems".

This paper proposes a power saving mechanism with a variable sleep period to reduce the power consumed by optical network units (ONUs) in passive optical network (PON) systems. In the PON systems based on time division multiplexing (TDM), sleep and periodic wake-up (SPW) control is an effective ONU power saving technique. However, the effectiveness of SPW control is fully realized only if the sleep period changes in accordance with the traffic conditions. This paper proposes an SPW control mechanism with a variable sleep period. The proposed mechanism sets the sleep period according to traffic conditions, which greatly improves the power saving effect. In addition, the protocols needed between an optical line terminal (OLT) and ONUs are described on the assumption that the proposed mechanism is applied to 10-Gbit/s (10G) class PON systems, i.e., IEEE 802.3av 10G-EPON and FSAN/ITU-T 10G-PON systems. The validity of the proposed mechanism is confirmed by numerical simulations.

Published as: R. Kubo, J. Kani, Y. Fujimoto, N. Yoshimoto, and K. Kumozaki, "Adaptive Power Saving Mechanism for 10 Gigabit Class PON Systems," IEICE Trans. Communications, Vol. E93-B, No. 2, pp. 280–288, Feb. 2010.

Papers Published in Technical Journals and Conference Proceedings

Electroluminescence and Capacitance-voltage Characteristics of Single-crystal n-type AlN (0001)/p-type Diamond (111) Heterojunction Diodes

K. Hirama, Y. Taniyasu, and M. Kasu

Appl. Phys. Lett., Vol. 98, No. 011908, 2011.

n-type single-crystal AlN (0001) layers were grown on diamond (111) substrates by metalorganic vapor phase epitaxy. We observed current-injected emission at a wavelength of 235 nm at room temperature in an n-type AlN/p-type diamond heterojunction diode. The emission is attributed to free-exciton recombination in diamond. From capacitance-voltage measurements of the n-type AlN/p-type diamond heterojunction, we determined that the AlN/diamond heterojunction exhibits the *staggered* (type-II) band alignment with a conduction band offset (ΔE_C) of 3.5 eV and a valence band offset (ΔE_V) of 4.0 eV.

Security of Cryptosystems Using Merkle-Damgård in the Random Oracle Model

Y. Naito, K. Yoneyama, L. Wang, and K. Ohta

IEICE Trans. Fundamentals, Vol. E94-A, No. 1, 2011.

Since the Merkle-Damgård hash function (MDFH) that uses a fixed input length random oracle as a compression function is not indifferentiable from a random oracle (RO) because of the extension attack, there is no guarantee of the security of cryptosystems that are

secure in the RO model when RO is instantiated with MDHF. This fact motivates us to establish a criteria methodology for confirming cryptosystem security when RO is instantiated with MDHF. In this paper, we confirm cryptosystem security by using the following approach: 1) Find a weakened random oracle (WRO) that leaks values needed to realize the extension attack. 2) Prove that MDHF is indifferentiable from WRO. 3) Prove cryptosystem security in the WRO model. The indifferentiability framework of Maurer, Renner, and Holenstein guarantees that we can securely use the cryptosystem when WRO is instantiated with MDHF. Thus, we concentrated on such finding a WRO. We propose the Traceable Random Oracle (TRO), which leaks values enough to permit the extension attack. By using TRO, we can *easily* confirm the security of the OAEP encryption scheme and variants of it. However, there are several practical cryptosystems whose security cannot be confirmed by TRO (e.g., RSA-KEM). This is because TRO leaks values that are irrelevant to the extension attack. Therefore, we propose another WRO, Extension Attack Simulatable Random Oracle (ERO), which leaks *just* the value needed for the extension attack. Fortunately, ERO is *necessary and sufficient* to confirm the security of cryptosystems under MDHF. This means that the security of *any* cryptosystem under MDHF is *equivalent* to that under the ERO model. We prove that RSA-KEM is secure in the ERO model.

Illuminant Color Estimation by Hue Categorization Based on Gray World Assumption

H. Kawamura, S. Yonemura, J. Ohya, and N. Matsuura

Proc. of the SPIE, Vol. 7873, pp. 787312–787312-12, San Francisco, USA, 2011.

This paper proposes a gray-world-assumption-based method for estimating an illuminant color from an image by hue categorization. The gray world assumption hypothesizes that the average color of all the objects in a scene is gray. However, it is difficult to estimate an illuminant color correctly if the colors of the objects in a scene are dominated by certain colors. To solve this problem, our method uses the opponent color properties that the average of a pair of opponent colors is gray. Thus, our method roughly categorizes the colors derived from the image based on hue and selects them one by one from the hue categories until selected colors satisfy the gray world assumption. In our experiments, we used three kinds of illuminants (i.e., CIE standard illuminants A and D_{65} and a fluorescent light) and two kinds of data sets. One data set satisfies the gray world assumption and the other does not. Experimental results show that estimated illuminants are closer to the correct ones than those obtained with the conventional method and the estimation errors for using CIE standard illuminants A and D_{65} in our method are within the barely noticeable difference in human color perception.

Optical Spectrum Control Circuit Using an Arrayed-waveguide Grating and Tunable Phase Shifters

K. Kato, Y. Ikuma, H. Takahashi, T. Mizuno, and H. Tsuda

IEICE Electronics Express, Vol. 8, No. 6, pp. 391–396, 2011.

We proposed and fabricated an optical spectrum control circuit using an arrayed-waveguide grating (AWG) and an array of channel waveguides with tunable phase shifters. We found that the spectral phase and amplitude of a modulated optical signal could be arbitrarily controlled if the number of channel waveguides was set to be more than twice the number of waveguides in the AWG. As a first demonstration, we successfully obtained a flat band-pass filter function with the fabricated device by controlling the tunable phase shifters to control the interference between the light propagating through them.

Efficient Combination of Likelihood Recycling and Batch Calculation for Fast Acoustic Likelihood Calculation

A. Ogawa, S. Takahashi, and A. Nakamura

IEICE Trans. Information and Systems, Vol. E94-D, No. 3, pp. 648–658, 2011.

This paper proposes an efficient combination of state likelihood recycling and batch state likelihood calculation for accelerating acoustic likelihood calculation in an HMM-based speech recognizer. Recycling and batch calculation are based on different technical approaches, i.e., the former is a purely algorithmic technique while the latter fully exploits the computer architecture. To accelerate the recognition process further by combining them efficiently, we introduce *conditional fast processing* and *acoustic backing-off*. Conditional fast processing is based on two criteria. The first criterion, *potential activity*, is used to control not only the recycling of state likelihoods at the current frame but also the precalculation of state likelihoods for several succeeding frames. The second criterion, *reliability*, and acoustic backing-off are used to control the choice of recycled or batch-calculated state likelihoods when they are contradictory in the combination and to prevent word accuracies from degrading. Large vocabulary spontaneous speech recognition experiments using four machines with different CPUs under two environmental conditions showed that, compared with the baseline recognizer, recycling and batch calculation (our combined acceleration technique) further reduced both of the acoustic likelihood calculation time and the total recognition time. We also performed detailed analyses to reveal each technique's acceleration and environmental dependency mechanisms by classifying types of state likelihoods and counting each of them. The analysis results confirmed the effectiveness of the combined acceleration technique.

Efficient Optical Flow Estimation Method Using Optimal Weighting Parameter of Sinusoidal Pattern

H. Sakaino

The Institute of Image Information and Television Engineers, Vol. 65, No. 3, pp. 382–394, 2011 (in Japanese).

In the Horn and Schunck optical flow method, a weighting parameter α of a motion smoothness constraint plays an important role in determining the estimation accuracy of optical flow. However, conventional methods of optimizing α have been based on an empirical selection or cross-validation, where a global optimization is done at a high computational cost. Thus, a more efficient optimization method is needed. We first assume that real images can be approximated by a two-dimensional sinusoidal wave function on the basis of an example of a previously used texture analysis. Two image features—the amplitude (standard deviation of image brightness) and wave number using the sinusoidal wave function—are used to analyze and model the relationship between the optimal α and two image features. From the analyzed model, the optimal α can be used to locally minimize the estimation error of optical flow. Because these two simple image features of given real images are used, the optimal α can be estimated efficiently. Experimental results for optical flow estimation accuracy show that our proposed method outperforms conventional optical flow ones.

A Rat Model for Measuring the Effectiveness of Transcranial Direct Current Stimulation Using fMRI

Y. Takano, T. Yokawa, A. Masuda, J. Niimi, S. Tanaka, and N. Hironaka

Neurosci Lett., Elsevier, Vol. 491, No. 1, pp. 40–43, 2011.

Transcranial direct current stimulation (tDCS) is one of the noteworthy noninvasive brain stimulation techniques, but the mechanism of its action has remained unclear. With the aim of clarifying the mechanism, we developed a rat model and measured its effectiveness using fMRI. Carbon fiber electrodes were placed on the top of the head over the frontal cortex as the anode and on the neck as the cathode. The stimulus was 400- or 40-μA current applied for 10 min after a baseline recording in an anesthetized condition. The 400-μA stimulation significantly increased signal intensities in the frontal cortex and nucleus accumbens. This suggests that anodal tDCS over the frontal cortex induces neuronal activation in the frontal cortex and in its connected brain region.

Word Alignment with Synonym Information

H. Shindo, A. Fujino, and M. Nagata

Information Processing Society of Japan, Vol. 4, No. 2, pp. 13–22, 2011.

We present a novel framework for word alignment that incorporates monolingual synonym knowledge to improve word alignment performance. We think that synonym information is helpful to overcome the data sparseness problem of word alignment since there are various lexical forms representing the same meaning in a bilingual corpus. However, synonym relations depend heavily on context or domain since a word in natural language is ambiguous. We designed a synonym probabilistic model with a topic model, which uses synonym information according to the context. Moreover, we propose a word alignment framework that jointly trains our synonym model and conventional bilingual model. The experimental results show that our proposed method obtained better results compared with cases where synonym or context information is not used.

Multi-sized Sphere Packing: Computational Modeling and Formulation for the Packing Density in Containers

S. Yamada, J. Kanno, and M. Miyauchi

Information Processing Society of Japan, Vol. 4, No. 2, pp. 23–30, 2011 (in Japanese).

This article provides a mathematical formula for determining the optimal sizes of two different sized spheres to maximize the packing density when randomized loose packing is used in containers with various shapes. The formula was evaluated with numerous computer simulations involving over a million of spheres.

Robust Semi-supervised Learning for Labeled Data Selection Bias

A. Fujino, N. Ueda, and M. Nagata

Information Processing Society of Japan, Vol. 4, No. 2, pp. 31–42, 2011.

We propose a robust semi-supervised learning method for designing good classifiers with a high generalization ability from labeled data whose distribution differs largely from that of test data in a target domain. Although JESS-CM is one of the most successful semi-supervised learning methods that achieved the best published results in natural language processing tasks, it has an overfitting problem in our task setting. We expect the proposed method to solve the overfitting problem by utilizing unlabeled data in the target domain with the labeled data for both training of discriminative and generative models composing a classifier. Our experimental results for text classification using three test collections confirmed that the classification performance obtained with the proposed method was better than that with JESS-CM in most cases of the task setting.

Non-data-aided Wide-range Frequency Offset Estimator for QAM Optical Coherent Receivers

T. Nakagawa, M. Matsui, T. Kobayashi, K. Ishihara, R. Kudo, M. Mizoguchi, and Y. Miyamoto

Proc. of OFC 2011, Vol. 2011, No. OMJ1, pp. 1–3, Los Angeles, USA.

We propose and experimentally demonstrate a novel blind frequency offset estimator for coherent quadrature amplitude modulation (QAM) receivers. Its frequency offset estimation range is more than three times the conventional estimation range.

Wide-range BER Measurement Scheme by Estimating BER of Discarded Frames for 10 G-EPON Systems

N. Ikeda, K. Terada, H. Uzawa, A. Miyazaki, S. Shigematsu, M. Urano, and T. Shibata

Proc. of OFC 2011, Vol. 2011, No. OTh, pp. OThT6, Los Angeles, USA.

This paper describes a new BER measurement method for obtaining the BER by estimating the number of error bits in discarded frames by using the rate of discarded frames. The BER is obtained precisely by the method.

Origin of Exciton Emissions from an AlN p-n Junction Light-emitting Diode

Y. Taniyasu and M. Kasu

Appl. Phys. Lett., Vol. 98, No. 131910, 2011.

Exciton emissions from an AlN light-emitting diode with an improved emission efficiency of 1×10^{-4}% were observed at 5.94 eV (208.7 nm) and 6.10 eV (203.2 nm) for current injection. The emission at 5.94 eV is attributed to an exciton emission originating from the crystal-field split-off valence band (CH-exciton emission). Owing to the large carrier-phonon interaction, the CH-exciton emission is accompanied by its phonon replicas. The emission at 6.10 eV is attributed to another exciton emission originating from heavy/light hole valence bands (HH/LH-exciton emission). From the emission energies, considering residual strain, the crystal-field splitting energy was determined to be −165 meV.

Measuring Sweeping Echoes in Rectangular Cross-section Reverberant Fields

K. Kiyohara, K. Furuya, Y. Haneda, and Y. Kaneda

Acta Acustica united with Acustica, Vol. 97, No. 2, pp. 278–283, 2011.

We investigated a new acoustical phenomenon, which we call sweeping echoes, in a two-dimensional (2D) space. Sweeping echoes in a three-dimensional (3D) space have recently been reported. We first investigated the regularity of reflected sound in a 2D regularly shaped space on the basis of number theory. The reflected pulse sound train has almost equal intervals between pulses on the squared-time axis as in a 3D space. This regularity of the arrival time of

reflected pulse sounds generates sweeping echoes whose frequencies increase linearly with time. Computer simulation of room acoustics shows good agreement with the theoretical results. We first describe our number-theory-based investigation of a square cross-section. Next, we describe rectangular cross-sections with various aspect ratios investigated using the same theory as used for the square. We also discuss our measurements of sweeping echoes in a long hallway. We propose a method for extracting the sweep rates of sweeping echoes by calculating their correlation with a time stretched pulse. We analyzed the sweeping echoes for a source and receiver at the center of a rectangular cross-section. These sweeping echoes were perceived not only at the exact center position but also around the center.

Underdetermined Convolutive Blind Source Separation via Frequency Bin-wise Clustering and Permutation Alignment

H. Sawada, S. Araki, and S. Makino

IEEE Trans. Audio, Speech, and Language Processing, Vol. 19, No. 3, pp. 516–527, 2011.

This paper presents a blind source separation method for convolutive mixtures of speech/audio sources. The method can even be applied to an underdetermined case where there are fewer microphones than sources. The separation operation is performed in the frequency domain and consists of two stages. In the first stage, frequency-domain mixture samples are clustered into each source by an expectation-maximization (EM) algorithm. Since the clustering is performed in a frequency bin-wise manner, the permutation ambiguities of the bin-wise clustered samples should be aligned. This is solved in the second stage by using the probability of each sample belonging to the assigned class. This two-stage structure makes it possible to attain good separation even under reverberant conditions. Experimental results for separating four speech signals with three microphones under reverberant conditions show the superiority of the new method over existing methods. We also report separation results for a benchmark data set and live recordings of speech mixtures.

Chapter 1. Integration of Statistical-model-based Voice Activity Detection and Noise Suppression for Noise Robust Speech Recognition

M. Fujimoto

Recent Advances in Robust Speech Recognition Technology, Bentham Science Publishers, 2011.

This chapter addresses robust front-end processing for automatic speech recognition in noisy environments. To recognize corrupted speech accurately, it is necessary to use methods that are robust against various types of interference. Usually, noise suppression is used for the front-end processing of speech recognition in the presence of noise. Voice activity detection (VAD) is also used for front-end processing to eliminate the redundant non-speech period. VAD and noise suppression are typically combined as series processing. VAD and noise suppression should not be assumed to be separate techniques because the output information of these methods is mutually beneficial. Thus, this chapter introduces the integrated front-end processing of VAD and noise suppression, which can utilize each other's input-output information.

Proposal of the Switching-control Algorithm for 3D-MEMS Optical Switch Module and Its Demonstration

M. Minakami, J. Yamaguchi, and S. Nemoto

The Japan Society for Precision Engineering, Vol. 77, No. 4, p. 383, 2011 (in Japanese).

A switching-control algorithm is necessary in order to connect the optical paths between input and output ports by using MEMS (microelectromechanical systems) mirrors in a free-space optical system. We propose a search algorithm that finds the maximum optical power by using the motion control technique of MEMS mirrors. We apply the algorithm to peak search control for optical path connection with maximum optical power and to optical power stabilization control in the case of environment changes, such as temperature change. The results confirm that the algorithm is suitable for practical use.

100Gb/s Ethernet Inverse Multiplexing Based on Aggregation at the Physical Layer

K. Hisadome, M. Teshima, Y. Yamada, and O. Ishida

IEICE Trans. Communications, Vol. E94-B, No. 4, pp. 904–909, 2011.

We propose a packet-based inverse multiplexing method to allow scalable network access with a bigger-pipe physical interface. The method is based on aggregation at the physical layer (APL) that fragments an original packet-flow and distributes the fragments among an adequate number of physical links or networks. It allows us to share wavelengths and/or bandwidth resources in optical networks. Its technical feasibility at the speed of newly standardized 100Gb/s Ethernet (100GbE) was successfully evaluated by implementing the inverse multiplexing logic functions on a prototype board. We demonstrated super-high-definition video streaming and huge file transfer by transmitting 100GbE MAC (media access control) frames over multiple 10GbE physical links via inverse multiplexing.

Multi-layer Hypercube Photonic Network Architecture for Intra-datacenter Network

T. Sakano, A. Kadohata, Y. Sone, A. Watanabe, and M. Jinno

IEICE Trans. Communications, Vol. E94-B, No. 4, pp. 910–917, 2011.

The popularity of cloud computing services is driving the boom in building mega-datacenters. This trend is forcing significant increases in the required scale of the intra-datacenter network. To meet this requirement, this paper proposes a photonic network architecture based on a multi-layer hypercube topology. The proposed architecture uses the cyclic-frequency arrayed waveguide grating (CF-AWG) device to realize a multi-layer hypercube and properly combines several multiplexing systems that include time division multiplexing (TDM), wavelength division multiplexing (WDM), wave-band division multiplexing (WBDM), and space division multiplexing (SDM). An estimation of the achievable network scale reveals that the proposed architecture can achieve a petabit-to-exabit-per-second-class, large-scale hypercube network with existing technologies.

Debating Diversity

M. Seyama

The Society of Polymer Science, Japan, Vol. 60, No. 5, p. 323, 2011 (in Japanese).

This paper provides comments about the debate on diversity and makes a suggestion.
